Renewable Energy 220 (2024) 119695

Contents lists available at ScienceDirect

Renewable Energy

journal homepage: www.elsevier.com/locate/renene

# Modeling, optimization, and economic analysis of a comprehensive CCHP system with fuel cells, reverse osmosis, batteries, and hydrogen storage subsystems Powered by renewable energy sources

Ali Dezhdar [a,b,**,1], Ehsanolah Assareh [c,d,*,1], Neha Agarwal [c,1], Alireza Baheri [d], Mehrdad Ahmadinejad [e], Narjes Zadsar [f], Ghazaleh Yeganeh Fard [f], Ali bedakhanian [g], Mona Aghajari [h], Maryam Ghodrat [i], Mohammad Mafizur Rahman [j], Moonyong Lee [c,***]

[a] Young Researchers and Elite Club, Dezful Branch, Islamic Azad University, Dezful, Iran
[b] Kimia Andimeshk Petrochemical Industries Company, Khuzestan-Iran
[c] School of Chemical Engineering, Yeungnam University, Gyeongsan 38541, South Korea
[d] Department of Mechanical Engineering, Dezful Branch, Islamic Azad University, Dezful, Iran
[e] Department of Mechanical Engineering, University of Vermont, Burlington, VT, USA
[f] Faculty of Mechanical Engineering, Alzahra University, Tehran, Iran
[g] Faculty of Energy Engineering, Shahrood University of Technology, Shahrood, Iran
[h] Department of Architecture, Semnan Branch, Islamic Azad University, Semnan, Iran
[i] School of Engineering and Information Technology, University of New South Wales Canberra, Canberra, 2610, ACT, Australia
[j] School of Business, and Centre for Health Research, University of Southern Queensland, Toowoomba, QLD, 4350, Australia

ARTICLE INFO

*Keywords:*
Combined cooling
Heating and power cycle
Optimization
Photovoltaic-thermal panel
Reverse osmosis
Fuel cells

ABSTRACT

Renewable energy sources are gaining significant interest due to their potential to decrease pollution resulting from the utilization of fossil fuels for generating electricity that is environmentally friendly. In this study, an innovative combined cooling, heating, and power cycle that makes use of geothermal, solar, and wind energy was examined. The 100 residential units are investigated throughout the year by a number of different subsystems, including photovoltaic-thermal panel, Wind Turbine, Steam Turbines, Fuel Cells, Heat pumps, Reverse Osmosis, Electrolyzer, batteries, and a hydrogen storage tank. The model of six European cities "Marseille, Monaco, Montpellier, Naples, Perpignan and Rome" located in Italy and France was the subject of this research. Transient assessment and the response surface method were employed in this study's optimization in TRNSYS. With the help of design of experiments, a few simulation scenarios were created, and response surface method was then utilized to examine the outcomes. Based on the findings, the optimal system greatly decreased the yearly life cycle costs of the boiler, the thermal comfort rating, the overall cost of consuming electricity, and the cost of natural gas consumption. The results demonstrate that the suggested system efficiency is increased by the addition of hydrogen storage and battery, and that the employment of fuel cells and WTs stabilizes the system's power output at all times of the day and night. According to the findings, Montpellier was the best city in terms of electricity generation, cost, and natural gas usage. The total amount of energy generated by the urban system over the course of a year is 425690.937 kWh/year, of which 121217.314 kWh/year are sold to the grid and the remainder is used to power homes. The annual use of natural gas is 47547.706 $m^3$/year, while the annual production of freshwater is 3756.07 $m^3$/year. The findings of the optimization showed that Montpellier's system, which includes 185 solar panels and 6 wind turbines, performs better than other systems.

* Corresponding author.School of Chemical Engineering, Yeungnam University, Gyeongsan 38541, South Korea.
** Corresponding author.Young Researchers and Elite Club, Dezful Branch, Islamic Azad University, Dezful, Iran.
*** Corresponding author.
*E-mail addresses:* ali.dezhdar@gmail.com (A. Dezhdar), Ehsanolah.assareh@gmail.com (E. Assareh), mynlee@ynu.ac.kr (M. Lee).
[1] These authors contributed equally to this article as the first authors.

https://doi.org/10.1016/j.renene.2023.119695
Received 13 April 2023; Received in revised form 28 October 2023; Accepted 18 November 2023
Available online 23 November 2023

**Nomenclature**

| | |
|---|---|
| $A$ | area ($m^2$) |
| $a$ | axial induction factor |
| $AOC$ | system's operating cost during a year ($) |
| $f$ | ON/OFF statues of a component (0 or 1) |
| $c$ | specific heat capacity (J/kg.K) |
| $d$ | discount rate |
| $E_{PV/T}$ | generated electricity by PV/T collectors (kJ/h) |
| EIR | energy efficiency ratio |
| $i$ | inflation rate |
| $hp_n$ | polynomial coefficients linking the load side $T_{db}$, $T_{wb}$, and supply side $T_{db}$ to the heating energy input ratio ($EIR_h$) of the heat pump |
| $f_{EER,h}$ | present fraction of rated heating energy input ratio |
| $f_{heat}$ | present fraction of rated heating capacity |
| $G_T$ | total solar radiation incident upon the collector surface ($kJ/hr.m^2$) |
| $h$ | Enthalpy (kJ/kg) |
| $I$ | current (A) |
| $I_C$ | initial investment cost ($) |
| LCC | life cycle cost ($) |
| $IAM$ | incidence angle modifier |
| $L_B$ | thermal load of inhabitants' body |
| $L$ | lenght (m) |
| $\dot{m}$ | mass flow rate (kg/h) |
| $n_{c,ser}$ | number of cells in series |
| $n_{m,ser}$ | number of modules in series |
| $n_f$ | number of factors |
| $n_L$ | lifespan (year) |
| $N_{tubes}$ | number of tubes in PV/T collector |
| $\dot{q}_{tot}$ | total cooling performed by the heat pump (kJ/h) |
| PMV | predicted mean vote |
| $PWF$ | present worth factor |
| $Q_{gen}$ | total heat produced by fuel cell |
| $\dot{q}_{sens}$ | sensible cooling performed by the heat pump (kJ/h) |
| $T$ | temperature (°C) |
| $tc_n$ | polynomial coefficients linking the load side $T_{db}$, $T_{wb}$, and supply side $T_{db}$ to the overall cooling capacity of the heat pump |
| $th_n$ | polynomial coefficients linking the load side $T_{db}$, $T_{wb}$, and supply side $T_{db}$ to the heating capacity of the heat pump |
| $U$ | voltage (V) |
| $R_I$ | resale income ($) |
| $x$ | factor |
| $y$ | response |

***Abbreviations***

| | |
|---|---|
| AFC | alkaline fuel cell |
| CCHP | combined cooling, heating, and power |
| DOE | design of experiments |
| HP | heat pump |
| PV | photovoltaic |
| PV/T | photovoltaic/thermal |
| RSM | response surface methodology |
| W | power |
| BFC | Auxiliary boiler fuel use |
| OEC | Overall Electricity Consumption |

*Scripts*

| | |
|---|---|
| $\eta$ | Efficiency |
| $a$ | air |
| $amb$ | ambient |
| $f$ | heat transfer fluid |
| $in$ | inlet |
| $out$ | outlet |

***Greek symbols***

| | |
|---|---|
| $\varepsilon_m$ | emissivity of the top surface of the collector |
| $\omega$ | absolute humidity ratio ($kg_{water}/kg_{air}$) |
| $\eta$ | efficiency |
| $\tau\alpha$ | transmittance-absorptance product for PV/T collector |
| $v$ | Wind speed (m/s) |
| $\rho_a$ | Air density ($kg/m^3$) |
| $\theta$ | angle of incidence (°) |

## 1. Introduction

The use of fossil fuels has led to climate change, air pollution and environmental destruction. Also, with the increase in population, the need for different energies, including electrical energy, cooling and heating, has also increased, and on the other hand, fossil resources are deteriorating and decreasing. There is a lot of interest in the use of various renewable energy sources [1,2]. Among the types of renewable energy and their benefits, numerous options can be considered: solar energy, because of its uniform distribution, wind energy, because of its high efficiency, and geothermal energy, because of its extensive global resources and lack of grid-scale energy storage requirements. Due to the great efficiency of this form of solar receiver and the simultaneous creation of electricity and heat, using solar energy and the absorption of this energy by solar systems like photovoltaic panels have received a lot of attention [3–5]. Integrating and using renewable energy sources in various cycles is conceivable. The interest in combined cooling, heating, and power (CCHP) cycles has grown significantly [6]. The CCHP is an effective method for the simultaneous delivery of thermal, cooling, and electrical energy, depending on the particular type of energy required [7]. Other benefits include less economic and environmental impacts than separate manufacturing systems [8].

For the heating and cooling load requirements of a housing complex, Kavian et al. created a hybrid photovoltaic-geothermal heat pump system. Using the particle swarm optimization technique implemented in MATLAB and TRNSYS, the system's performance was optimized in order to get the best possible results. The findings indicate that a polycrystalline hybrid PV/T system with a solar share of 31 % is a more ideal solution from an economic and environmental standpoint, with a 3-year return on investment [9]. Wang et al. investigated the discrepancy between demand and energy supply in CCHP cycles using a dynamic interaction technique. The optimization findings demonstrated that their approach enhanced the operational and economic performance of the cogeneration systems [10]. Ren et al. presented two distinct hybrid CCHP systems using natural gas, solar energy, geothermal energy, the grid, and electricity, and three buildings were modelled. The findings indicate that system A, which comprises of all components with the exception of solar thermal photovoltaic panel, has higher benefits. This is supplied for each of the three structures. In addition, the system design and component capacity are dependent on the kind of building [11]. Musharavati et al. investigated the transformation of a simple refrigeration system into a multigenerational system, which included an absorption chiller, an organic flash cycle, solar panels, and a reverse osmosis subsystem. The thermal modelling findings for this system demonstrated that its energy efficiency, exergy efficiency, and net output power were 5.46 %, 20.16 %, and 70.85 kW more than a typical system [12]. Li et al. investigated a unique system that blends the conventional CCHP cycle with a wind energy and hydrogen supply to

address the two concerns of decarbonization of the transportation system and power system sustainability. The findings of the economic and energy performance analysis revealed that, compared to conventional systems, this innovative method reduced costs and carbon dioxide emissions by 72 % and increased energy efficiency by the same amount. The largest amount of hydrogen produced by this system throughout the winter was 500 kg [13].RSM optimization was used by Mahdavi et al. to calculate the ideal number of PV/T for a solar system. The results demonstrated that the regression models supplied by the RSM for calculating the net power and efficiency of the system were quite accurate. The data also showed that the system's overall production power was 61.73 MW, and its exergy efficiency was 44.22 %. Several research on the utilization of renewable energy to produce various energies, including electricity, have been carried out recently [14]. Dezhdar et al. presented a novel strategy in 2023 to combine solar energy with ocean thermal energy to supply the thermal energy needed for an organic Rankine cycle for generating electricity. This mechanism was started using the water temperature difference in the dam and the area's ability to absorb solar radiation energy. Iran's Karkheh Andimeshk Dam was the subject of a case study on climate change, and its system included two solar panels, an organic Rankine cycle, and a thermoelectric generator to boost its efficiency in generating power [15]. Power generation, as previously stated, is crucial for many places of the world. As a result, Chen et al. proposed a hydrogen production system in 2021. This system was built using solar thermal energy absorption and ammonia-based chemical energy storage. In order to provide a new method in solving renewable systems, a new method with a fresh approach compared to previous articles was presented for the first time by High thermal freshwater electrolysis and ammonia-based chemical thermal energy storage (using a solid oxide electrolyzer cell) [16]. In 2022, Alrobaian introduced a multiple energy production system, and this system was designed dependent on how well the photovoltaic absorbs sun's radiation, and this system consisted of two power generation units, the Brayton cycle and the Kalina cycle, as well as a cooling production unit by an absorption chiller. The findings indicated that in order to bridge the disparity between the absorption chiller rate of production and the subscriber's cooling requirement, the planned power station should be linked to the national grid and supply the rest of the user's needs from it. The exergy efficiency of the power plant was reported to be 42.11 % [17]. Saikia et al. carried out an optimization in 2021 to produce a reliable solar panel electrolyzer that would increase hydrogen generation. Tn this work, eleven operating parameters were selected for optimization using an orthogonal array, and it was established that the highest production of hydrogen was 319.35 Ncm3/hr. The Taguchi technique was then employed, and it was determined that the maximum production of hydrogen was 645.89 Ncm3/hr, up 50.56 % from the greatest production value achieved from the orthogonal array [18].

In 2023, Ji et al. optimized multi-cycle renewable energy systems with hydrogen and battery energy storage. The results showed that the renewable energy systems with hydrogen storage and battery storage are 21.5 % and 5.3 % cheaper than the renewable energy systems without energy storage [19]. In 2023, Güven and Mengi evaluated meta-heuristic algorithms in determining the dimensions of hybrid energy systems by examining renewable energy systems with hydrogen storage features. This study presents a complex framework focusing on the optimization of hybrid energy systems and energy flow management, with an emphasis on energy modules, such as wind, solar, biomass gasification, and fuel cells. Excess energy is converted into hydrogen for storage and then used in fuel cells [20]. In 2013, Modu et al. conducted a systematic review of hybrid renewable energy systems with hydrogen storage. In this research, it was stated that the disadvantages of batteries are their large size, limited lifespan, and high cost. For this reason, energy planners are looking to hydrogen-based storage systems as a potential solution [21]. In 2023, Liu et al. evaluated the performance of wind-solar-hydrogen systems for renewable energy production and green hydrogen production and storage. The results show that this system has the potential to produce 931.39 kg of hydrogen per year with an energy efficiency of 16.03 % and an exergy efficiency of 17.94 %. The integration of multiple renewable energy sources and hydrogen production in the system increases the utilization rate of renewable energy and provides a promising solution for sustainable energy production and use [22]. In 2023, Abedi et al. investigated solar desalination chimneys and investigated the feasibility of integrating solar chimneys with dehumidification systems. Numerical simulations show that small-scale integrated solar chimney desalination systems can be placed on the roof of a residential building and produce about 600 L of fresh water per day to supply fresh water for a household [23].

In 2022, Khani et al. investigated a new multigeneration system based on solar energy and desalination-humidity-dehumidification. The results show that solar energy integration increases the Rankine cycle electricity generation from 37.3 % (winter) to 59.41 % (summer), while the overall electricity generation increases by 18 kW compared to the base case scenario [24]. In 2023, Tawalbeh et al. analyzed a hybrid photovoltaic/solar chimney for a seawater desalination plant. A complete parametric study was also conducted for the integrated system with a transparent solar panel to evaluate the effect of different parameters on air velocity, static pressure, mass flow rate, air temperature inside the chimney, and turbine output power under solar radiation of 850 W/m2. The effect of radiation on turbine and PV power output was investigated. The results of the current model showed that the net output power and freshwater production for the hybrid system reached 261 kW and 8.867 kg/s, respectively [25]. In 2023, Assareh et al. conducted a transient simulation for a new solar-geothermal cogeneration system by selecting heat transfer fluids using thermodynamic analysis and intelligent modeling. The system consists of parabolic solar collectors, a steam Rankine cycle, a steam Rankine cycle with an organic Rankine cycle, a proton exchange membrane electrolysis, and a reverse osmosis desalination unit. Maximizing energy efficiency and reducing cost rate were selected as two objective functions and determined using a multi-objective sorting genetic algorithm (NSGA-II). The proposed system produces 1140 kW of electricity in the optimal state, and in the best state, the energy efficiency is 32.39 % and the cost is $36.32/GJ [26].

A survey of the relevant literature, as noted above, finds the following gaps in knowledge.

- The ideal integrated CCHP system's simultaneous utilization of solar, wind, and geothermal energy has not been researched.
- A solar-wind-geothermal CCHP system that combines energy storage and hydrogen generation has not been shown to work well in transitory situations.
- RSM is not described as a statistical or mathematical technique to lower CCHP system expenses over the long run.

One issue that has received less attention in the past researches is the use of renewable systems to provide energy for residential buildings. Today, providing the energy needed by residential houses, including electricity, cooling and heating, should be considered as one of the essential things in studies, and new systems pay attention to the ability to supply buildings and residential units to provide the energy needed by people. The systems based on renewable energies need more complete studies, because the transition from fossil resources to renewable resources requires a strong scientific support, and the design and launch of new systems requires complete and comprehensive information on technical and environmental conditions, equipment types, Feasibility and design. The development of energy systems with high performance and reducing environmental pollution as well as reasonable cost is of great importance. In this regard, in this research, to address this issue, an innovative system in which various renewable energies have been used to produce the energy needed by residential complexes has been proposed.

Therefore, this research combined energy storage and hydrogen

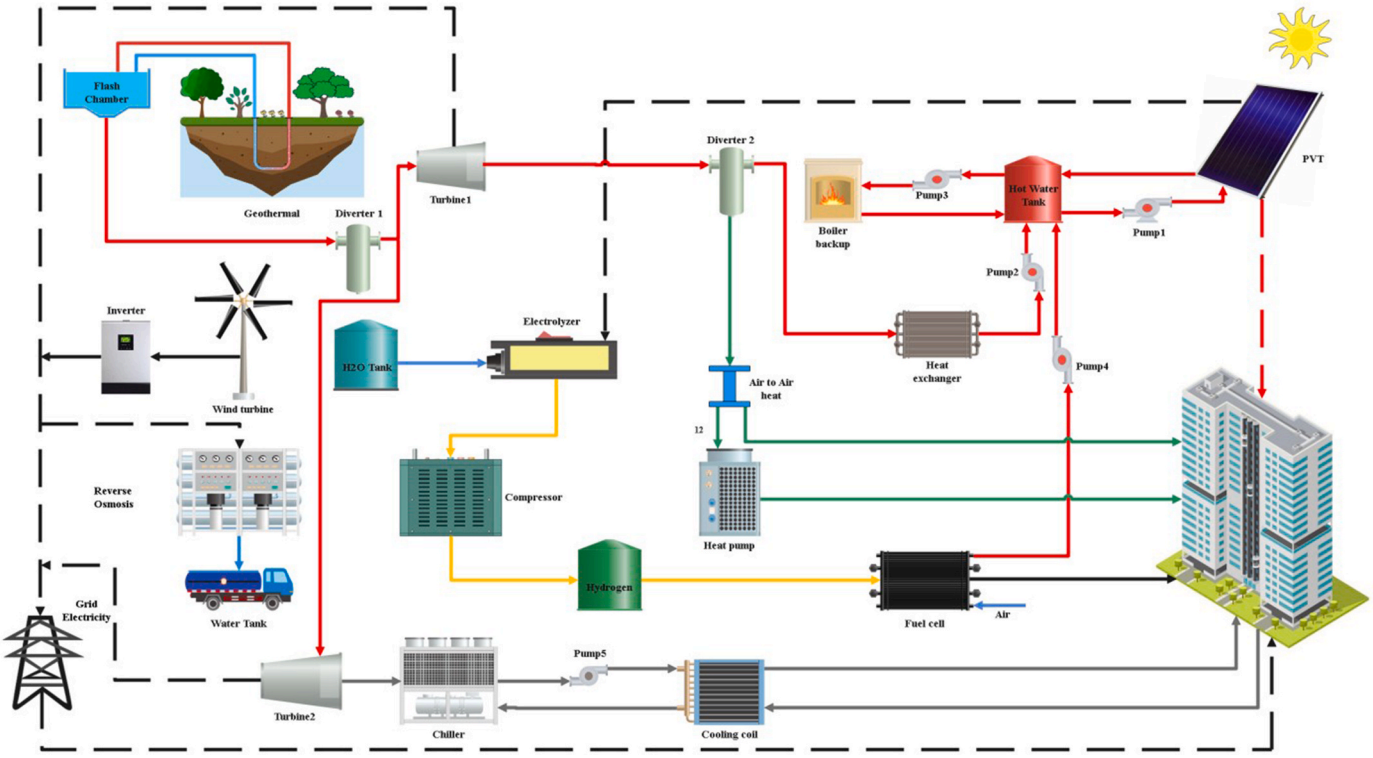


**Fig. 1.** The proposed CCHP system.

production to build and optimize a planned CCHP system using a mix of solar-wind and geothermal energy. A heat pump (HP), steam turbine (ST), fuel cell, solar panel, geothermal loop, wind turbines (WTs), reverse osmosis systems, and electrolyzer units are a few of the important subsystems that make up the proposed system. The planned system is configured to handle the electrical loads, domestic hot water use, and cooling and heating demands of 100 residential units. The quantity of solar cells, wind turbines, fuel cells, HP capacity, and jet turbine power were all taken into consideration as important elements for evaluating the system's performance. The energy and financial metrics selected for evaluation comprise the electricity and natural gas consumption of the boiler, the projected average vote (PMV) used to assess thermal comfort, and the life cycle cost (LCC) chosen as a monetary measure. The unique feature of this work is the simultaneous investigation of the effects of the design parameters of the planned system's economic and energy metrics from a transient statistical viewpoint.

In short, the current work activities are as follows.

- A novel approach is being proposed for integrating photovoltaic/thermal panel units, fuel cell units, and wind turbines in order to enhance the overall efficiency of the system, while also mitigating system costs and promoting environmental sustainability through the utilization of renewable resources.
- The application of a multi-objective optimization technique is being utilized to determine the optimal conditions for system performance.
- The optimization process will involve selecting the response level optimization method.
- The feasibility and reliability of deploying the system across various regions of Europe will be thoroughly assessed.

## 2. Overview of the proposed renewable energy system

A schematic of the planned CCHP cycle is shown in Fig. 1. This cycle consists of solar panel (PV/T), geothermal loops, water turbines, fuel cells, electrolyzers, reverse osmosis, HPs, batteries, and ST, among other parts and subsystems. During the course of a year, the intended system will provide electricity, heating, cooling, hot water, and fresh water to the 100 residential units. Solar panel (PV/T), fuel cell, wind turbine (WT), and solar thermal subsystems are in charge of power production in this system. The WTs and fuel cell are regarded to satisfy the matching demand and serve as a backup and stabilize electricity production throughout the night if the PV/T subsystem's power output is insufficient to meet the system's demands. A battery serves a portion of the system's requirements in addition to these subsystems. The unpredictable nature of ST power production is caused by the variable exhaust gas temperature. The geothermal well releases steam, which enters the ST and produces electricity. Following that, the output of the turbine is transmitted to the heat pump (HP), whose purpose is to provide the system with the necessary thermal energy for heating and cooling. The electrolyzer uses some of the system's electricity to produce hydrogen, which is then stored in a hydrogen storage tank for use in the fuel cell. Reverse osmosis uses some of the WT generating power to create fresh water. The solar panel and fuel cell units, which are two units of electricity and heat generation, along with the equipment of the steam boiler, supply the amount of hot water needed by the system. Moreover, these three units are linked to the storage tank via three cold water outputs and three heated water inlets. The storage tank's inlet and outlet temperatures are designed and managed in such a way that they satisfy the requirements of residential units day and night.

The creation of renewable energy involves high initial investment costs and low ongoing maintenance expenses, which gives it a different structure from technologies used to produce fossil fuels. The initial investment expenses are comparatively low for techniques of producing energy from fossil sources. In the following, the equations governing the multiple energy production system will be examined and the relationships and equations governing the thermodynamic modeling of the equipment used in the system will be explained with the TRNSYS software in order to provide a complete understanding of the problem for how to calculate the results.

### 2.1. System analysis and modeling

The suggested system under discussion is simulated with TRNSYS utilizing a new approach. The TRNSYS software environment, which is built on graphics and used to model the behavior of transient systems, is particularly adaptable. TRNSYS may be used to simulate various dynamic systems, even though the majority of simulations are geared toward analyzing the performance of thermal and electrical energy systems. The TRNSYS and TESS libraries were used for modelling as a result of their dependability [27] and complete validation [28–34] in prior experimental experiments.

#### 2.1.1. Steam turbine

Type 592 is used from the TESS library, which works with the approach of isentropic efficiency and back pressure of the steam turbine. Users of this kind may select up to five injection ports and five extraction ports along the turbine's length. The model may be given with the steam conditions at these ports in any sequence, and the type will arrange them properly depending on the stream pressure. In order to match the streams' pressures with the turbine's local pressure, the turbine will automatically put the injection and extraction streams at the appropriate points throughout its length. Eq. (1) describes the work done during the current stage of growth [35].

$$\dot{W}_{GT}=\dot{m}_{in}\left(h_{in}-h_{out,actual}\right) \tag{1}$$

#### 2.1.2. Solar panel

The Type 560 is designed to represent an unglazed solar panel (PV/T) with integrated photovoltaic (PV) cells that serves as both a source of electricity and heat for a fluid stream flowing via tubes attached to an absorber plate below the PV cells. This model depends on linear relationships between the PV cells' efficiency and their temperature and incoming solar energy. Calculating the power generated by the solar panel (PV/T) and output temperature is done using equations (2) and (3) [36]:

$$E_{PV/T}=(\tau\alpha)_n\cdot IAM\cdot G_T\cdot A\cdot\eta_{PV/T} \tag{2}$$

$$T_{f,out}=\left(T_{f,in}+\frac{\varepsilon_m}{\kappa}\right)\exp\left(\frac{N_{tubes}}{\dot{m}_f c_f}\frac{\kappa}{\theta}L\right)-\frac{\varepsilon_m}{\kappa} \tag{3}$$

#### 2.1.3. Wind turbine

TRNSYS Type 90 was employed to model the wind turbines (WTs) in the study. The model, as described in equations (4) and (5) [37], accounts for variations in air density and wind speed at different heights when calculating the power output of a wind energy conversion system (WECS) based on its power versus wind speed curve. In other words, the model takes into consideration the impact of changes in air density and wind speed with height on the power output of the WTs [37].

$$E_{WT}=\rho_a C_P A_r v^3 \tag{4}$$

$$C_P=4a(1-a)^2 \tag{5}$$

In the equation, the variables that are used are air density, wind turbine rotor area, wind speed, and the wind turbine power factor. The wind turbine power factor also takes into account the axial induction value. The maximum power coefficient is also included in the equation, and it is referred to as the maximum power factor. The value of the maximum power factor, according to Betz's limit, is 59.3 %. Betz's limit is a theoretical maximum limit for the amount of energy that can be extracted from the wind by a wind turbine. It indicates that no wind turbine can extract more than 59.3 % of the kinetic energy available in the wind.

#### 2.1.4. Heat pump

The research uses a heat pump for heating and cooling. Energy efficiency ratio (EIR) represents the delivered power to the device's design capacity when operating at nominal settings [38]. Actual heating capacity coefficient is the ratio of heat output to the heat input by the heat pump, indicating its efficiency in converting input power to heat output [39].

$$f_{heat}=th_1+th_2T_{wb,in}+th_3T_{wb,in}^2+th_4T_{db,amb}+th_5T_{db,amb}^2+th_6T_{wb,in}T_{db,amb} \tag{6}$$

The EIR coefficient in heat pump heating operation is calculated as follows [39]:

$$f_{EIR,h}=hp_1+hp_2T_{wb,in}+hp_3T_{wb,in}^2+hp_4T_{db,amb}+hp_5T_{db,amb}^2+hp_6T_{wb,in}T_{db,amb} \tag{7}$$

#### 2.1.5. Fuel cell

The alkaline fuel cell (AFC) is simulated numerically using TRNSYS Type 173. The model assumes that air is present on the cathode side. The electrochemical model is based on an empirical correlation, which is used to determine the current-voltage characteristic at the standard operating temperature. Although a calculation of the AFC-heat stack's production is made, a comprehensive dynamic thermal model is not. Equations (8)–(11) are used to calculate stack power, cell voltage, module and stack respectively [40].

According to equation (12) [41], the energy efficiency of the fuel cell was computed by taking into account the cell voltage, the enthalpy of hydrogen at standard conditions, the number of electrons, and Faraday's constant. Eqs. (13) and (14), respectively, were used to compute the fuel cell's hydrogen consumption and total heat production [40].

$$U_{cell}=\frac{U_{mod}}{n_{c,ser}} \tag{8}$$

$$U_{mod}=U_0-b\log(I_{stack})-R_{ohm}I_{stack} \tag{9}$$

$$U_{stack}=n_{m,ser}U_{mod} \tag{10}$$

$$E_{stack}=U_{stack}I_{stack} \tag{11}$$

$$\eta_E=\frac{U_{cell}.n_e.F}{\Delta_{H_2}} \tag{12}$$

$$\dot{V}_{H_2}=\frac{n_{c,ser}n_{m,ser}I_{FC}}{zF\rho_{gas}}S_{H_2}\eta_F \tag{13}$$

$$Q_{gen}=E_{stack}\left(\frac{1-\eta_E}{\eta_E}\right) \tag{14}$$

#### 2.1.6. Electrolyzer

The behavior of the electrolyzer was simulated using the mathematical model TRNSYS Type 160 for a high-pressure alkaline water electrolyzer. Fundamental thermodynamics, heat transport theory, and actual electrochemical interactions serve as the model's foundations. The number of cells linked in series determines the electrolyzer's total hydrogen production rate, which may be estimated as follows [39–43]:

$$\dot{n}_{H_2}=\eta_f N_{cells}\frac{I_{ely}}{nF} \tag{15}$$

#### 2.1.7. Battery

Pb-accumulators are mathematical representations of lead-acid batteries, often referred to as lead-acid batteries. In this model, resistance (in relation to concentration-overvoltage) and capacity are connected via a straightforward equivalent circuit. Based on both current losses and polarization effects, this model fits a range of chargers with differing capacity and calculates the equilibrium voltage at various amounts of charge (when charging and discharging) [27].

**Table 1**
coefficients for the rate-relationship of fresh water.

| Coefficient | Value |
|---|---|
| p3 | 130.2 |
| p2 | 183.2 |
| p1 | 0.06739 |
| q1 | 867.3 |

**Table 2**
The initial solution conditions.

| Input | amount | Unit | Reference |
|---|---|---|---|
| *Steam turbine efficiency* | *0.90* | - | [35] |
| *Volume of hot water tank* | *16.4* | $m^3$ | [38] |
| *Fuel consumption* | *Natural gas* | - | [39] |
| *Combustion efficiency (auxiliary boiler)* | *0.86* | - | [39] |
| *Set point temperature (auxiliary boiler)* | *65* | °C | [39] |
| *PV/T slope* | *32* | ° | [42] |
| *System life* | *25* | *Years* | [43] |
| *Electrode area of alkaline fuel cell* | *0.01* | $m^2$ | [53] |
| *The last gas storage tank pressure* | *399* | *Bar* | [53] |
| *Gas storage tank volume* | *50* | $m^3$ | [53] |
| *HP Bypass Deficiency* | *0.1147* | - | [55] |
| *HP heating energy ratio* | *0.255* | - | [55] |

**Table 3**
Basic information of the apartment unit.

| Item | Unit | Value (unit) | Reference |
|---|---|---|---|
| *Wallstotal heat transfer coefficient* | $\frac{W}{m^2k}$ | *0.51* | [42] |
| *Roofoverall heat transfer coefficient* | $\frac{W}{m^2k}$ | *0.316* | [42] |
| *Floortotal heat transfer coefficient* | $\frac{W}{m^2k}$ | *0.318* | [42] |
| *WindowsHeat transfer coefficient* | $\frac{W}{m^2k}$ | *3.1* | [42] |
| *Roof height* | *m* | *2.8* | [52] |
| *Number of windows* | - | *3* | [52] |
| *Window area* | $m^2$ | *4* | [53] |
| *The total area of the windows of every unit* | $m^2$ | *12* | [53] |
| *The amount of absorption of solar radiation in the walls* | - | *0.61* | [53] |
| *Solar absorptance of roof* | - | *0.61* | [53] |
| *Total area of each unit* | $m^2$ | *196* | [53] |
| *Occupants* | *People* | *4* | [63] |
| *Total floor area* | $m^2$ | *19600* | - |
| *Total occupants* | *People* | *400* | - |

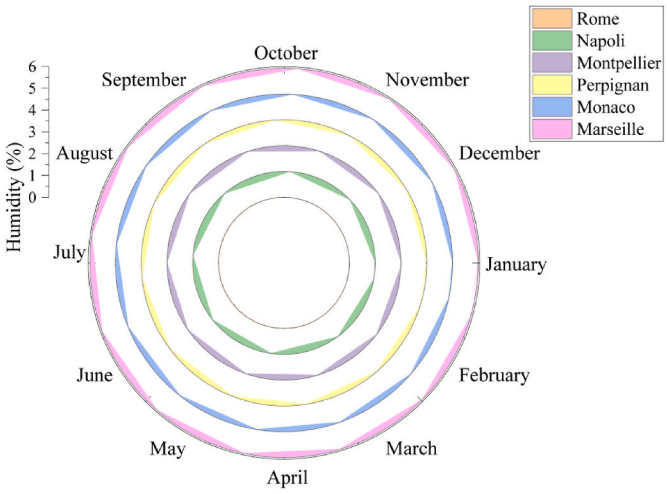


**Fig. 3.** Yearly variation in the environment's relative humidity.

### 2.1.8. *Reverse osmosis*

Equation (16) was used to compute the steam cycle pump's output power [44–46]:

$$\text{PumpPower} = (\dot{W}_{net}) \times 1.79 \tag{16}$$

Equation (17) was used to calculate the freshwater rate.

$$\text{Fresh Water Rate} = \frac{(p1 \times PumpPower^2 + p2 \times PumpPower + p3)}{(PumpPower + q1)} \tag{17}$$

In this study, the production rate of freshwater is measured in cubic meters per hour. Table 1 contains the coefficients for the equation of 17 [44–46].

Due to the sheer amount of formulae, the governing formulas of the other parts of the new CCHP cycle, such as storage containers and auxiliary boilers, are not included here, even though they are taken into account throughout the computations. You may find these formulae in the literature [39–43]. The settings and input values used to model the major subsystems are shown in Table 2. To calculate the electricity purchase rate from the entire electricity distribution network, the electricity sales rate and the natural gas purchase tariff were used based on the data of Dongellini and Morini [47].

## 2.2. *Building*

An apartment complex with two building and 12 and 13 stores and 4 flats on each level serves as the subject of the study. There are 100 apartments in all, and each one is a normal apartment with a 196 m2 floor space [48]. Table 3 displays each unit's specs. Using the approach

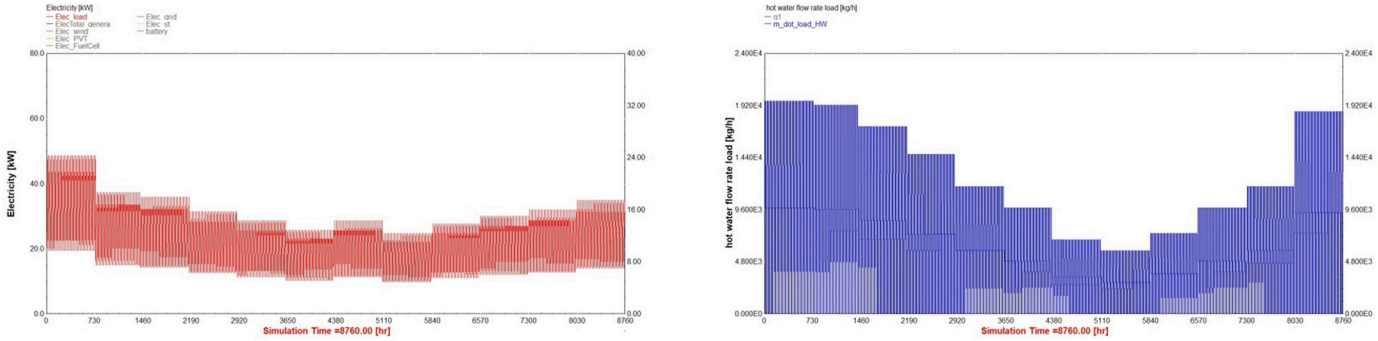


(a) (b)

**Fig. 2.** Specifications of the required load of the complex. (a) Amount of electricity required; (b) required hot water rate.

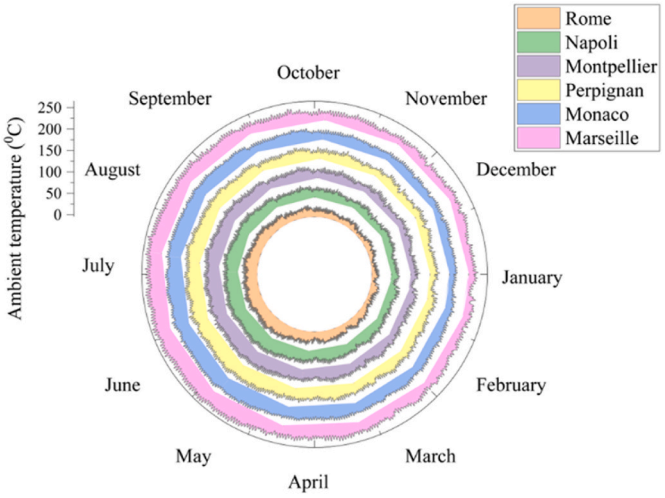


**Fig. 4.** Temperature of the chosen environment throughout the year.

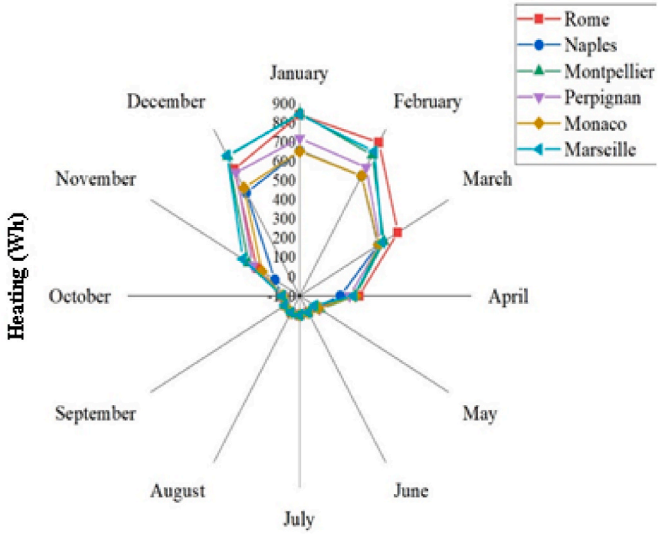


**Fig. 5.** Heating loads of the selected case study.

outlined in Refs. [49,50], the characteristics of hourly electricity and hot water usage for an apartment complex over the course of a year have been computed and are shown in Fig. 2.

The quantity of power needed in the six cities under study for a year is shown in Fig. 2 (a). These results have been calculated for 8760 h of electrical energy required by residential units, and the need for cooling and heating equipment used in this system to produce cooling and heating in hot and cold seasons is provided by the system itself. Fig. 2 (b) depicts the amount of hot water used annually in the cities of Rome, Monaco, Montpellier, Naples, Perpignan, and Marseille. As the results show, in the cold seasons of the year, due to the need for heating load due to the heater of residential units, the amount of hot water increases, and in the hot seasons of the year, due to the decrease in the need for heating load, the amount of hot water production has decreased, and the lowest Hot water is produced in July.

Fig. 3 shows the average monthly relative humidity of the six cities. The proportion of water vapor partial pressure to water vapor pressure at a particular temperature is known as relative humidity. Relative humidity depends on the temperature and pressure of the measured system. At a colder temperature, the same amount of water vapor results in higher relative humidity.

As the results show, the months of June, July, and August during the summertime have the highest average relative humidity for six cities., and the lowest average relative humidity of the six study cities was recorded in the months of December, January, and February in the winter season. Also, the city of Naples has the highest relative humidity and the lowest relative humidity relative to the city of Marseille.

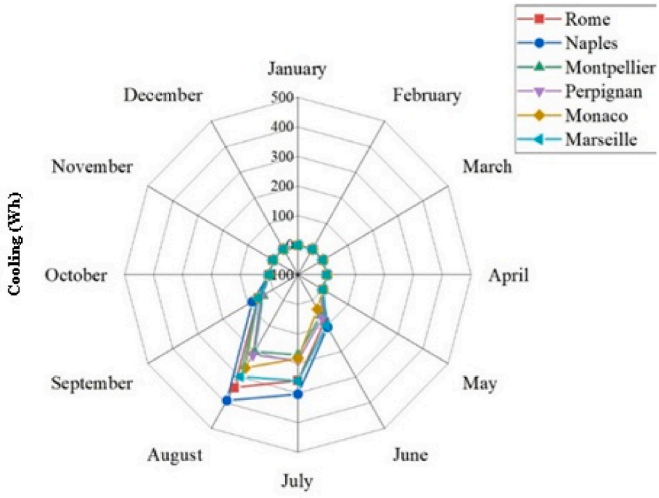


**Fig. 6.** Annual cooling loads of the selected case study.

Fig. 4 shows the average monthly temperatures of the six cities. The highest and lowest temperatures for the city of Rome were 36.8 and −2.4, respectively, 33.14 and 1.4 for Monaco, 35.4 and −4 for Montpellier, 36.05 and −1.35 for Naples, 35.8 and −2.65 for Perpignan, and 35.75 and −3.65 for Marseille. The findings indicate that for six cities, the summertime and the months of June, July, and August had the highest average ambient temperatures, and the lowest ambient temperature of the six study cities is recorded in December, January and February in the winter season.

In Fig. 5, it can be seen that the amount of heating required for one year in the cities of Rome, Monaco, Montpellier, Naples, Perpignan, and Marseille was $2.41 \times 10^6$, $1.92 \times 10^6$, $2.4 \times 10^6$, $1.77 \times 10^6$, $2.11 \times 10^6$, and $2.4 \times 10^6$, respectively. The amount of cooling required for one year in the cities of Rome, Monaco, Montpellier, Naples, Perpignan, and Marseille were $5.49 \times 10^5$, $4.01 \times 10^5$, $3.47 \times 10^5$, $6.52 \times 10^5$, $3.83 \times 10^5$, and $5.26 \times 10^5$, respectively (Fig. 6). Therefore, as shown, the need to provide cooling is much less than the need for heating.

As the results show, due to the cold weather in winter and autumn, the need for heating load increases, and the highest heating rate is recorded in the months of December, January, and February. As the ambient temperature increases, the need for heating load decreases. Due to the cold air of Rome, the highest heating load is related to this city, and due to the higher air temperature of Monaco, the lowest heating load is related to this city. It should be noted that the results of the heating load are the inverse of the ambient temperature.

As the results of Fig. 6 show, due to hot weather in summer and spring, the need for cooling load increases in these seasons for six study cities, and the highest cooling load is recorded in June, July and August. As the ambient temperature increases, the need for cooling load increases. Due to the high ambient temperature of Naples, the amount of cooling load required by Naples city is higher than other studied cities, and due to the lower air temperature of the city of Montpellier, the lowest cooling load is related to this city. It should be noted that the results of the cooling load are directly related to the ambient temperature.

### 2.3. Case study

In this study, the system's performance was evaluated by examining

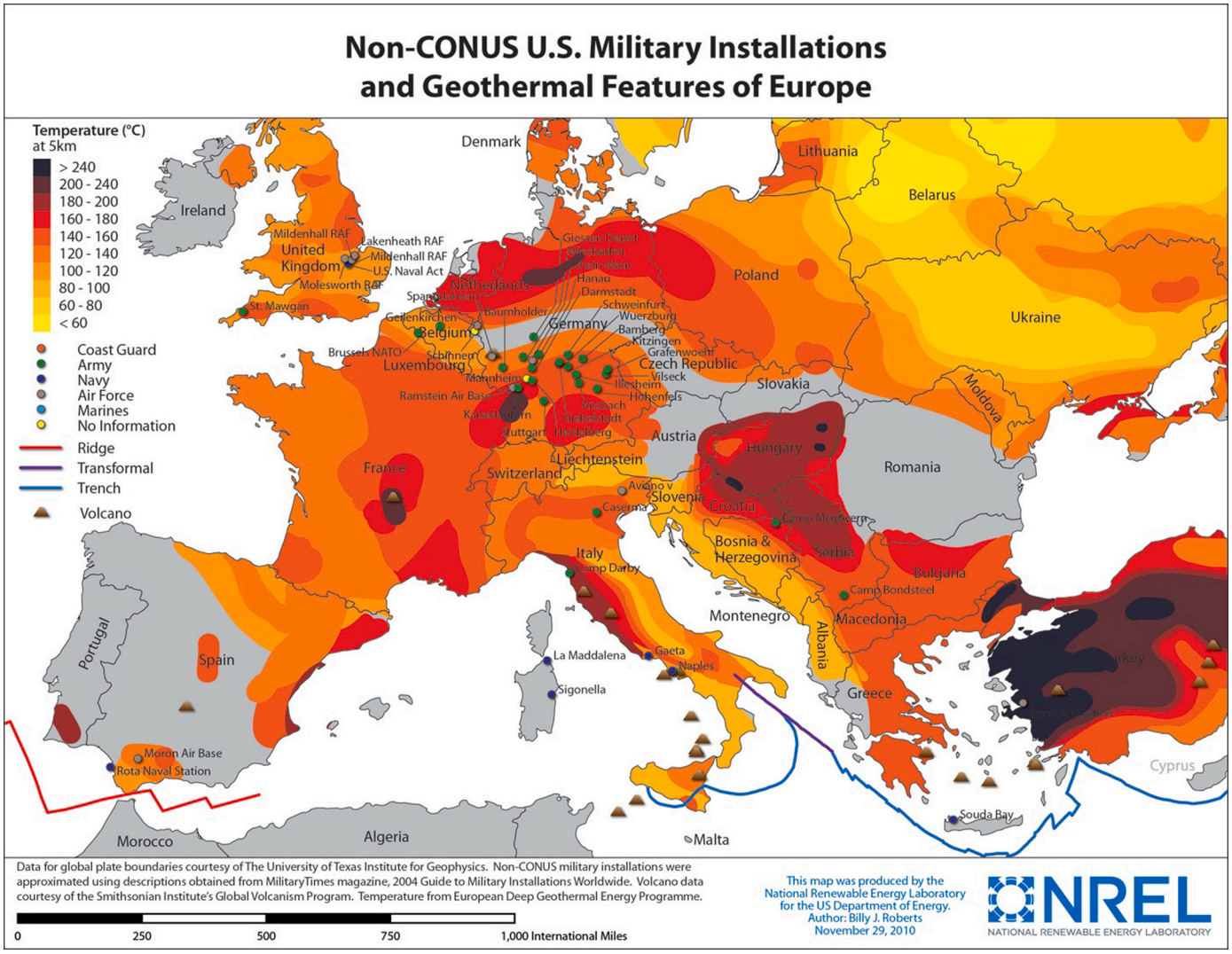


**Fig. 7.** Geothermal map of Europe [64].

the effects of weather patterns from various locations. The six European cities of Monaco, Montpellier, Marseille, Perpignan, Rome, and Naples were included in the research region. The geothermal, wind, and solar maps of the chosen sites are shown in Figs. 7 and 8. Monaco is a tiny nation on Western Europe's Mediterranean Sea, on the French Riviera, a little distance west of the Italian province of Liguria. Monaco has moderate winters and hot, dry summers due to its Mediterranean environment. Solar and geothermal energy are two examples of renewable energy sources that are presently utilized in Monaco, as seen in Figs. 7 and 8. A city in southern France called Montpellier is situated 10 km inland from the Mediterranean Sea. Short, hot, dry, and mainly clear summers and lengthy, chilly, windy, and partly overcast winters are the norm in Montpellier. Solar and geothermal energy are two of the renewable energy sources being utilized in Monaco. Cities in southern France include Marseille and Perpignan. Their Mediterranean environment has hot, sunny summers and moderate, comparatively damp winters. The availability of wind and solar energy was one of the parameters that led to the selection of Marseille and Perpignan. Italy's capital is Rome. Winters in Rome are lengthy, cold, humid, and partially overcast, while summers are brief, hot, humid, dry, and largely clear. More than a third of the electricity generated in Rome comes from green sources including solar photovoltaics, wind energy, and geothermal energy. Italy is the third biggest generator of renewable energy in Europe. After Rome and Milan, Naples is the third-largest city in Italy and serves as its regional capital. Naples has short summers that are hot, muddy, dry, and mainly clear and lengthy winters that are chilly, rainy, and partially overcast. Among the renewable energy sources employed in Naples are solar and geothermal energy [64,65].

The first findings are shown in Fig. 9. The findings indicated that Marseille produced more power than the other cities. Economic studies also shown that this approach was more efficient in Marseille. Naples and Marseille both had better comfort levels (PMV) and boiler gas use. As a result, this city was chosen for more research.

## 3. Parametric study

The impact of changing HP heating capacity on target performance is shown in Fig. 10. Theoretically, it is true that increasing the heating capacity raises costs; this has been shown. Additionally, the impact on the power generated is negatively correlated with the increase in total heating capacity. The findings demonstrate that as heat pump capacity increases, less electricity is produced because the heat pump requires more electrical energy. The system's power production provides the heat pump with the electrical energy it needs to operate. Also, when the heat pump's capacity grows and this unit produces more cooling and heating, the system's expenses rise.

The impact of changing HP cooling capacity on the desired performance is appeared in Fig. 11. Costs go up when cooling capacity is

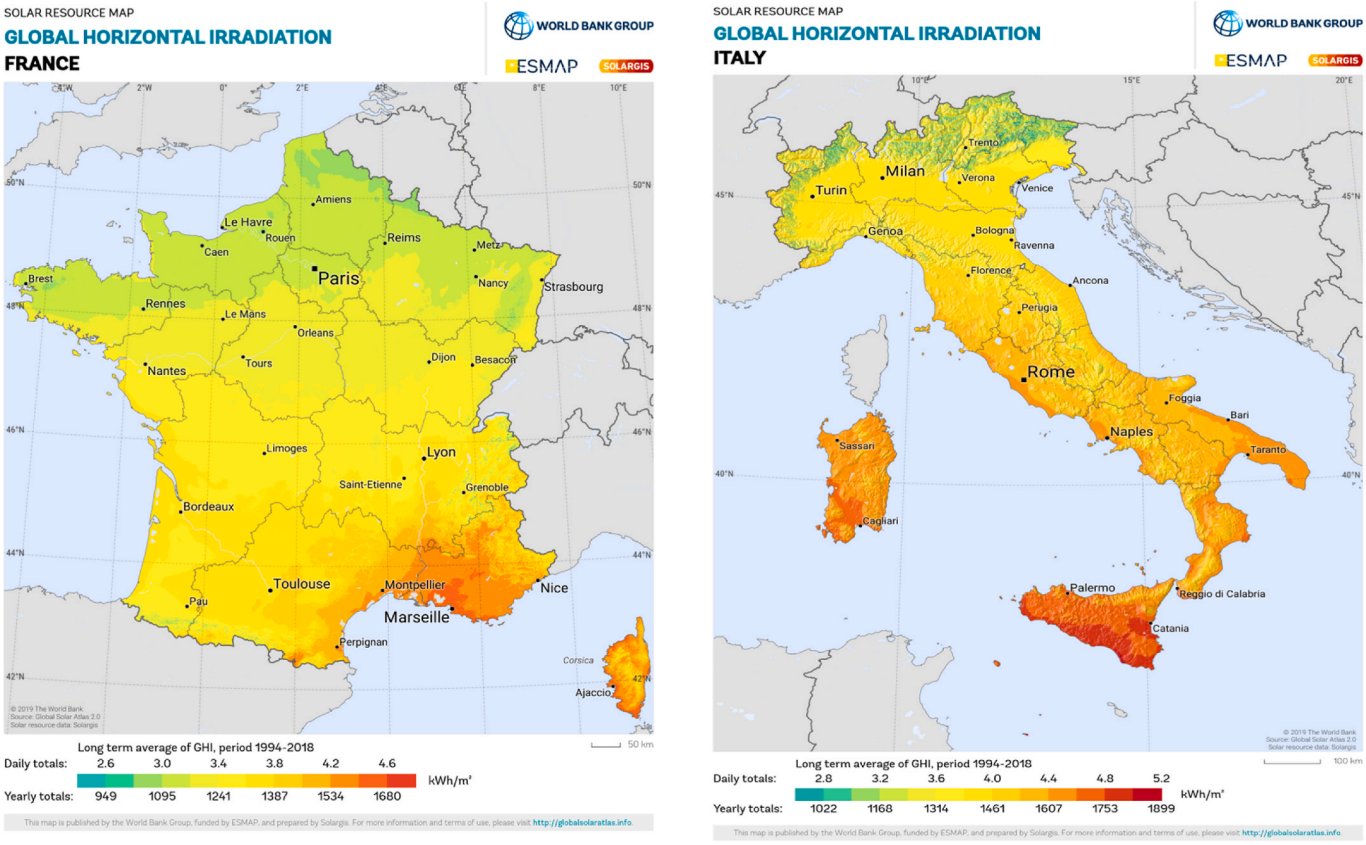


Global horizontal irradiation [65]

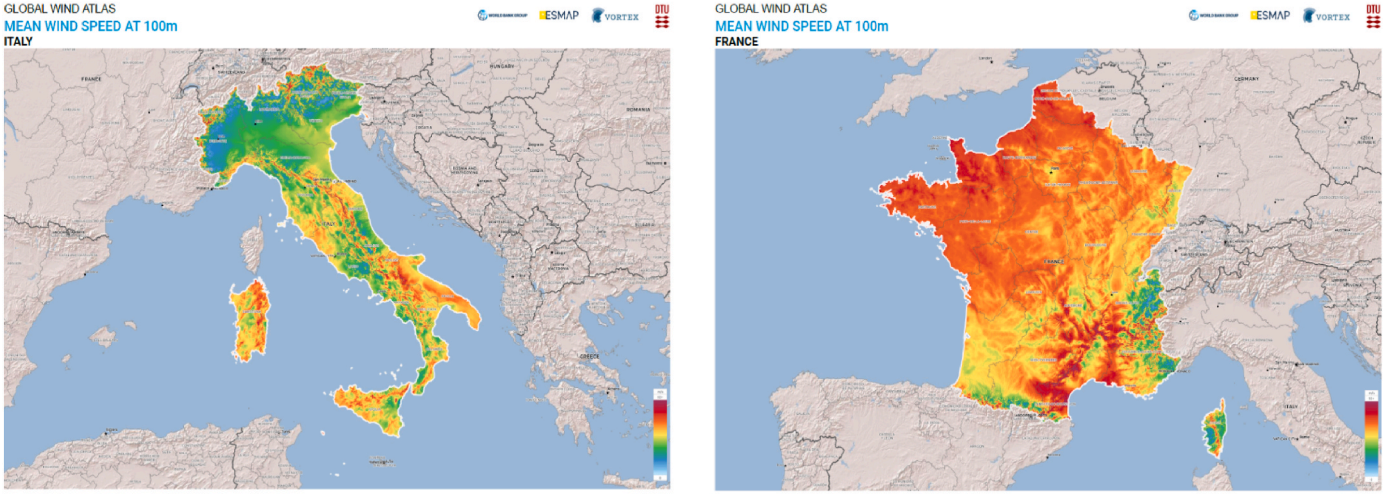


The Global Wind Atlas [66]

**Fig. 8.** Solar (Top) and wind (Down) maps of Europe [65,66].

increased. Additionally, a rise in cooling capacity has a detrimental effect on the cycle's ability to generate power, which results in a drop in output. As the results show, with the increase of the cooling capacity, the amount of electricity produced decreases, because the need of cooling for electric energy increases. The system generates the electrical energy needed for the cooling unit, which influences the system's overall output of electricity. Also, the price for the suggested renewable system will rise as a result of the heat pump unit's increased cooling capacity and subsequent rise in cooling output.

Fig. 12 illustrates how variations in the fuel cell unit's power level affect the objective functions. The results show that increasing fuel cell power increased the system's total power but also increased the system's cost. However, since a fuel cell is utilized in the proposed system to manage the generation of electricity during periods when the wind and sun are not present, it is feasible to lower the system's costs by maximizing its capacity. A fuel cell is basically a device that converts used

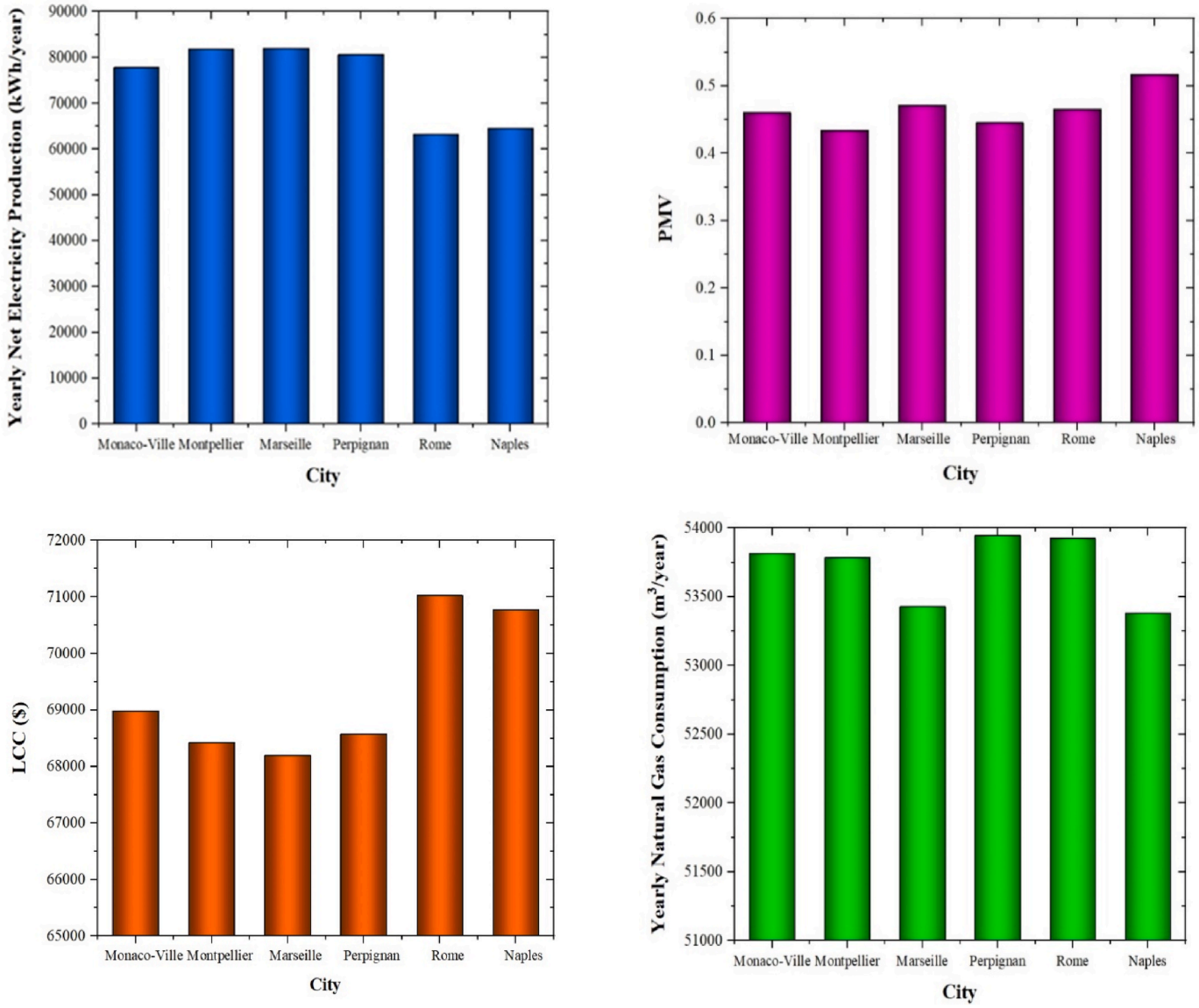


**Fig. 9.** Comparison of cities in the initial state of the proposed system.

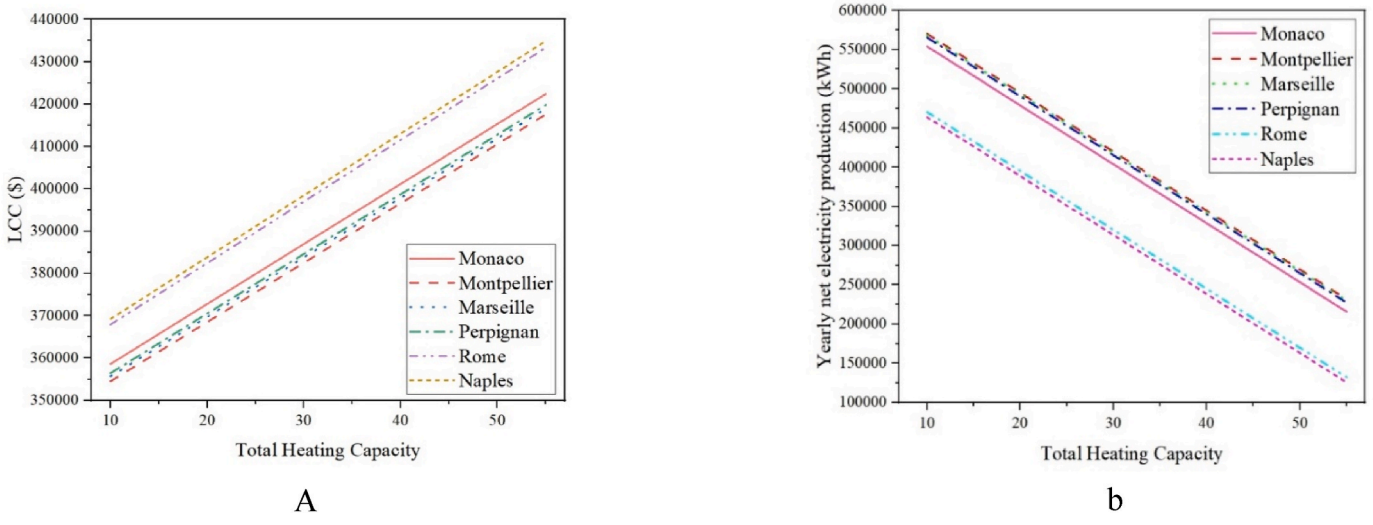


**Fig. 10.** Effects of raising the device heat pump's rate heating capacity.

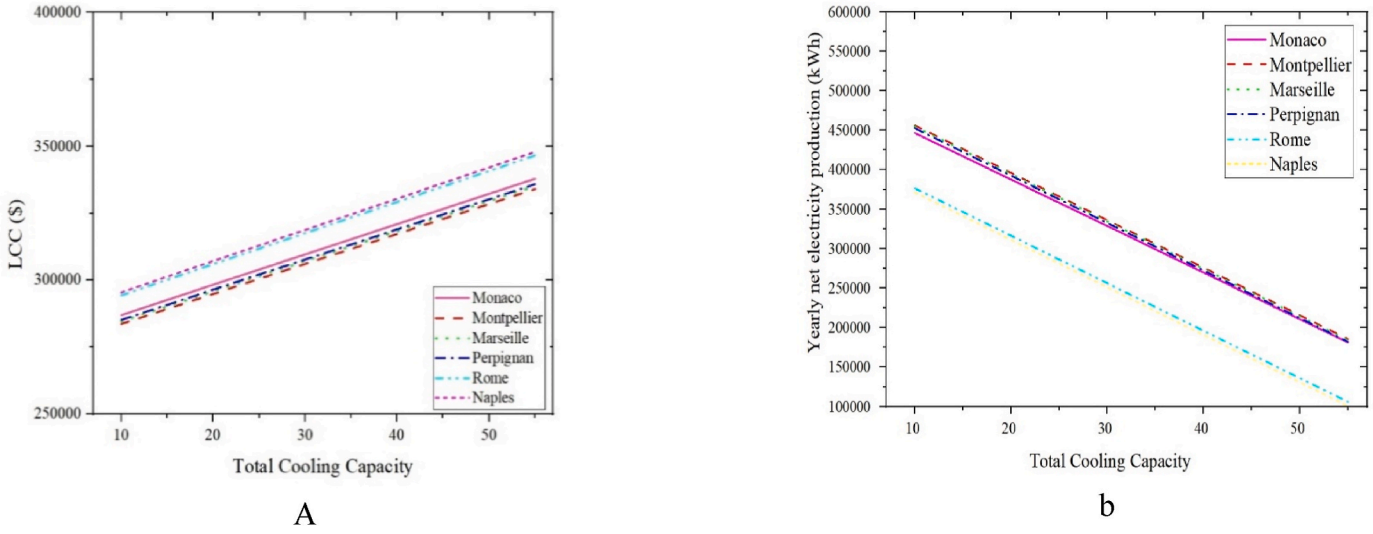


**Fig. 11.** Effects of raising the unit heat pump's rate cooling capacity.

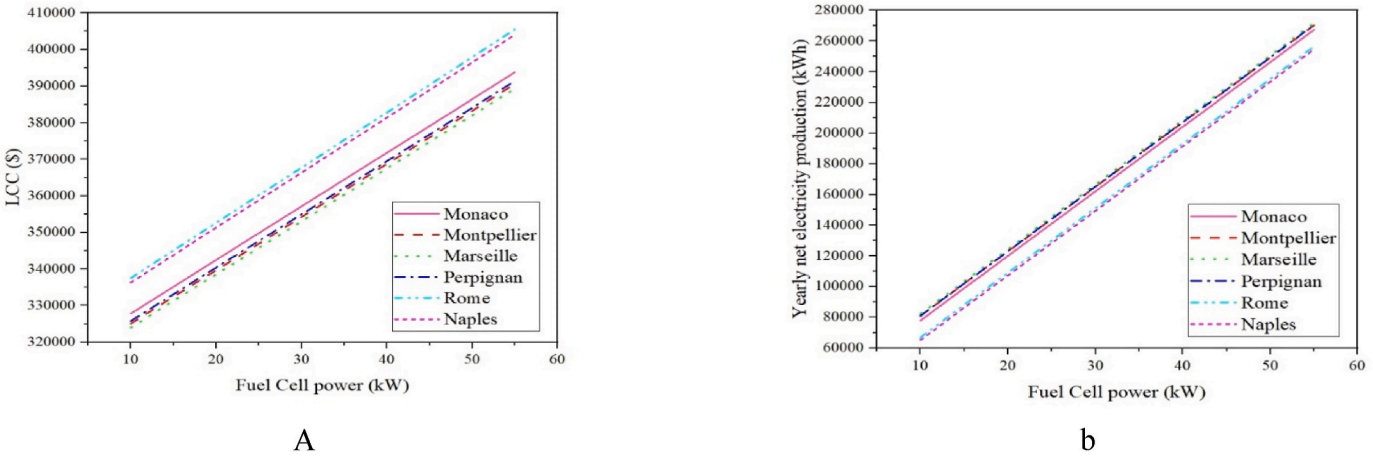


**Fig. 12.** Effect of increasing the fuel cell capacity on the target functions (produced electricity and total cost).

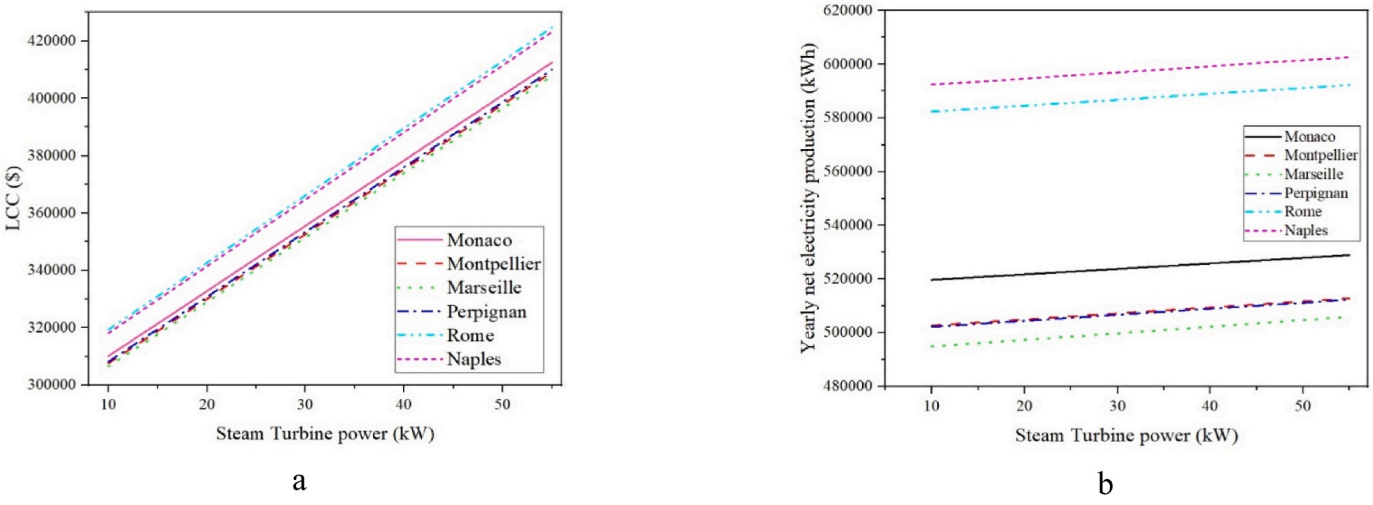


**Fig. 13.** Effect of increasing the steam turbine capacity on the target functions (produced electricity and total cost).

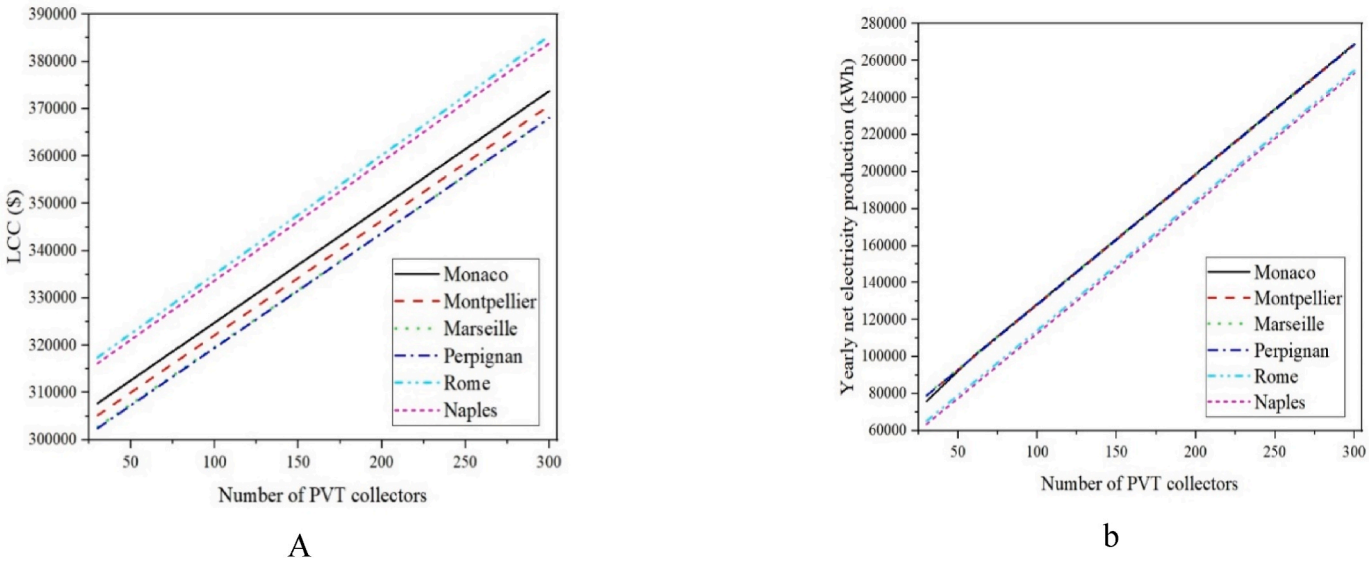


**Fig. 14.** Effect of the number of solar panel on the objective functions (produced electricity and total cost).

fuel such as hydrogen, natural gas, etc. into electricity, water and heat. In other words, a fuel cell is similar to a battery, but unlike a battery, it does not need a charge storage. As long as the fuel and air required by the battery are supplied, the system will work. By increasing the fuel cell's power, the cost of the unit rises owing to the need for more fuel, but because the unit performs better with more fuel, the amount of energy produced by the unit also rises, and as a consequence, the cost of the unit decreases. Moreover, the overall system's output power rises.

A steam turbine is a power generation device that takes thermal energy from steam and turns it into rotational motion. The impact of ST power adjustments on the objective functions was examined, as shown in Fig. 13. The findings showed that system expenses and energy generation rose when ST power increased. The capacity of the ST was decreased to an acceptable level, and the expenses were decreased, by balancing the quantity of power needed by the system and waiting for the suggested design of the ST. By increasing the capacity of the steam turbine, the heat flow hits the turbine blades with high speed and pressure and causes the turbine to rotate at the desired speed. The turbine can produce the required power according to the capacity and rotation speed. The operation of the steam turbine is based on the law of conservation of energy, according to which the heat of the fluid passing through the turbine is converted into work and only the structure and form of energy changes.

Fig. 14 depicts how changes in the PV/T (number of solar panels) affect the objective functions. The results showed that as the number of solar panels rose, so did the cost; however, as the number of panel increased, so did the amount of power generated. In this type of solar receiver, the heat produced in the photovoltaic panel when using sunlight to generate electricity is transferred to the heat storage tank using a circulating pipe and a heat exchanger module. At the same time, the working temperature of the photovoltaic module is reduced to improve its photoelectric conversion efficiency. The heated end of the tank then distributes the hot water to the user. Next, the electrical energy produced by photovoltaic can be used. For this reason, with the increase in the number of solar panels, the energy absorbed by the sun increases, and hence by supplying the thermal energy needed by the panels, the amount of electricity produced and also the heat produced by this type of solar unit also increases. But it should be said that solar equipment is one of the expensive equipment, the cost of buying them is high, but the cost of maintenance and maintenance of these units is low. As a result, the cost of the entire system rises as the quantity of solar panels does as well. Solar panels produce electricity and heat by absorbing solar

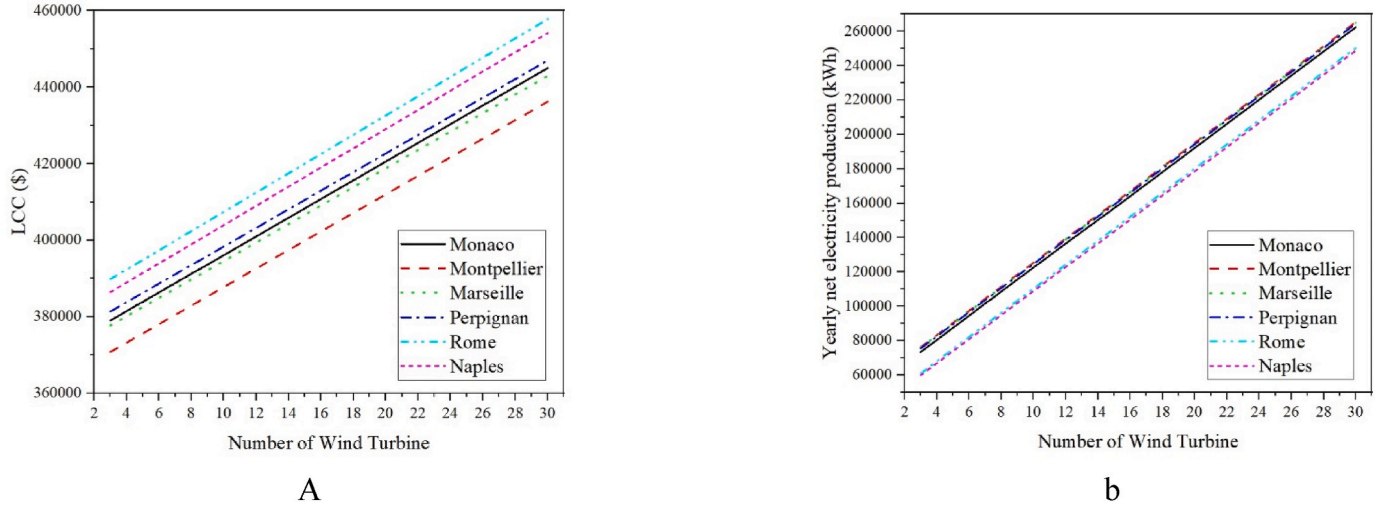


**Fig. 15.** The impact of wind turbine number on the objective functions (produced electricity and total cost).

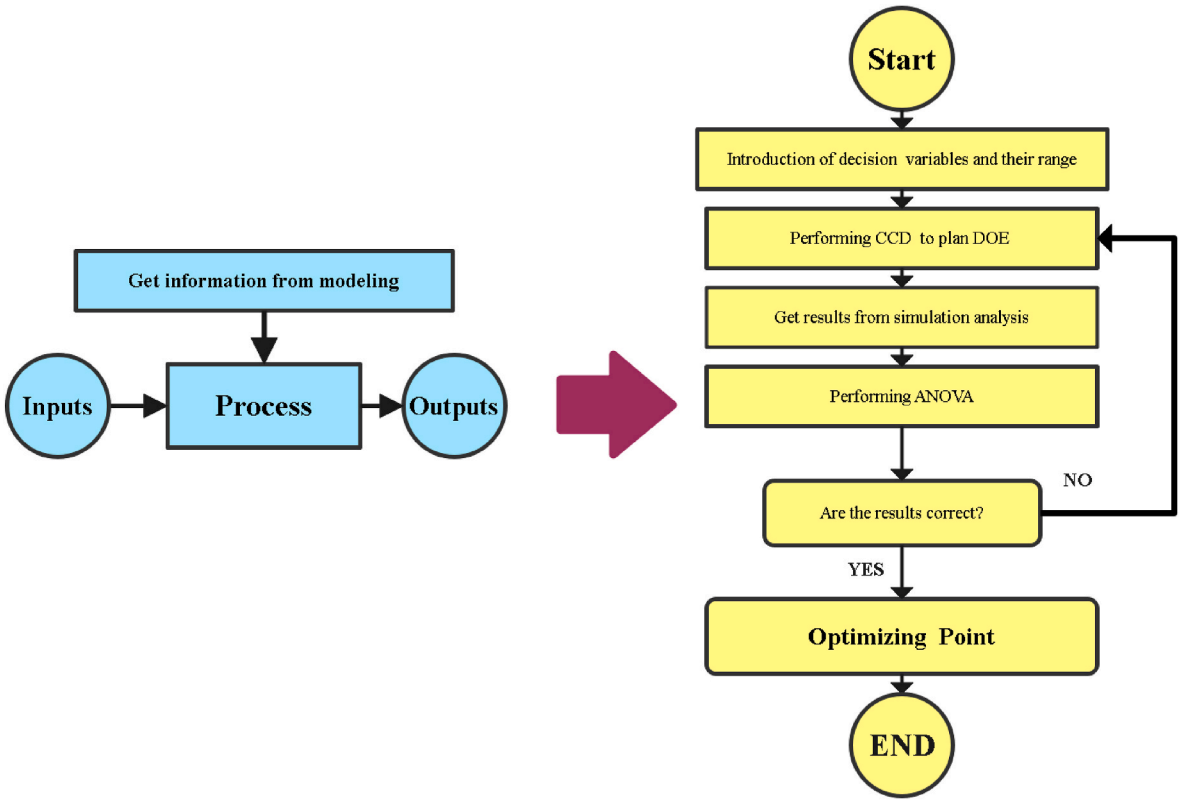


**Fig. 16.** Flowchart of the response surface method.

energy. As the number of solar panels increases and the solar farm expands, the amount of electricity and heat produced by the solar farm made of thermal photovoltaic panels also increases. On the other hand, the cost of the solar farm will increase by expanding it due to the initial costs including the purchase of equipment and installation.

In Fig. 15, it was examined how changes in the number of WT impacted the target functions. The results indicated that as the number of WTs climbed, so did the cost of the system and the amount of power produced. The kinetic energy of the wind is transformed into mechanical energy and ultimately into electrical energy in wind turbines. Wind turbines can be combined with solar cells for optimal use and production of more power. Because of this, as the number of wind turbines rises, so does the wind turbines' capacity to collect energy from the wind and their ability to circulate their blades, and as a result, by providing the wind energy required by the wind turbine, the amount of electricity produced by this type of electricity generation unit also increases. But it must be said that wind turbines are considered expensive equipment, the cost of their purchase is high, but the cost of maintenance and maintenance of these units is low. In consequence, the cost of the entire system rises as the number of wind turbines does. Wind turbine produces electricity by absorbing wind energy. The wind turbines used in this research are horizontal axis type. As the number of wind turbines increases and the wind farm expands, the amount of electricity produced by the wind farm from horizontal axis wind turbines also increases. On the other hand, the cost of the wind farm increases by expanding it due to the initial costs including the purchase of wind turbine equipment and their installation and operation.

**Table 4**
Decision variables and limited decision variables.

| *design variable* | *Lower limit* | *Upper limit* |
|---|---|---|
| *Solar panel* | *0 (–)* | *250 (–)* |
| *Wind turbines* | *0 (–)* | *15 (–)* |
| *steam turbinecapacity* | *0 (kW)* | *90 (kW)* |
| *fuel cellcapacity* | *0 (kW)* | *70 (kW)* |
| *HPcooling capacity* | *0 (kW)* | *70 (kW)* |
| *HPheating capacity* | *0 (kW)* | *80 (kW)* |

## 4. RSM (response surface methodology)

Some real-world problems require identifying and analyzing the impact of input variables on the response variable. Selecting the finest member from a group of feasible members is referred to as optimization. In its most basic form, it is attempted to determine its maximum and lowest value by methodically choosing data from a set that is readily available and computing the value of a real function. One of the practical methods for modeling and solving these problems is response surface methodology. A collection of statistical methods and applied arithmetic are used in response surface methodology to create empirical models. Response procedure designs aim to maximize the response, which is affected by a number of independent variables. The response surface method has steps to implement and these steps are presented in Fig. 16. First, the studied system is defined and the input variables to the system are identified. Then the main variables are entered into the RSM test design system and the output responses are evaluated, analyzed and optimized based on the input variables. After conducting the tests and identifying the effective factors, according to the application of the response surface methodology, the relationship between the variables related to the effective input factors and the response level variable is determined using a non-linear regression model. Then the optimal value of each of the nonlinear model variables is obtained using the ideal programming method.

RSMs establish links between performance measures and several design variables, called factors. The purpose of RSM is to create an optimal combination of components. The advantage of the RSM method compared to the old methods is to reduce the number of modeling for a more organized and integrated examination of the elements, as well as the possibility of combining factors with selected simulations [60].Using

equation (18) as a general model of second-order RSM, The general model can be described as follows:

$$y = r_0 + \sum_{i=1}^{n_f} r_i x_i + \sum_{i=1}^{n_f} r_{ii} x_i^2 + \sum_{i<j=2}^{n_f} \sum r_{ij} x_i x_j \quad (18)$$

In this model, the coefficients are extracted through regression analysis, which displays the response, the factor and the number of factors. A CCHP cycle is modelled and optimized using six factors, as shown in Table 4. A is determined as the number of solar panels since area of the panel has an effect on the total electricity production of a system and its fuel consumption. Power generation and system costs are also greatly affected by the number of wind turbines. As a result, factor B was the number of wind turbines. Among the three power generation subsystems, steam turbine capacity was selected as the C factor. A significant part of the electricity required for modeling is produced by the fuel cell subsystem, so factor D reflects the fuel cell's power. Because the proposed system is cooled and heated with a heat pump, the E and F factors are the cooling and heating capacities. As shown in Table 4, the selected factors have experienced a wide range of changes. The range of change of all factors is from the lower limit of zero to the upper limit, where the value of zero indicates the non-use of these components, and the upper limit is selected based on installation restrictions and maximum cooling and heating loads. According to the range of factor changes, RSM and CCD methods provided 52 performances. Finally, Design Expert software [61] was used for the statistical calculations needed for the simulation data.

In this research, 4 objective functions were considered to optimize the technical and economic performance of the system, and the relationships of the four objective functions investigated, which include total electricity consumption (OEC), boiler fuel consumption (BFC), predicted average vote (PMV) and LCC is reviewed in order below [39,48,49]. The target functions are intended to reduce system cost, increase system efficiency in electricity production, reduce boiler fuel consumption to prevent the increase of system costs in fuel supply, as well as reduce environmental issues and predicted average vote to provide thermal comfort for residential units. And it should be stated that the purpose of this research is to introduce a high-power system to supply energy to residential houses at a suitable economic cost [39,48–51,54,56–59].

$$OEC = \frac{\sum_{i=1}^{n_t} \left(E_{loadprofile} + E_{HP} + E_{elctrolyzer} + E_{pumps} + E_{compressor} - E_{PV/T} - E_{fuelcell} - E_{WTs}\right)}{3600 \times \frac{1}{\Delta t}} \quad (19)$$

$$BFC = \frac{\sum_{i=1}^{n_t} \left(\dot{m}_f c_f \left(T_{setpoint} - T_{f,inlet}\right) . f_{boiler}\right)}{\eta_{boiler} LHV} \quad (20)$$

$$PMV = [0.303 \cdot \exp(-0.036M) + 0.028] \cdot L_B \quad (21)$$

$$LCC = I_C + PWF \cdot AOC - R_I \quad (22)$$

$$PWF = \begin{cases} \frac{1}{d-i}\left[1 - \left(\frac{i+1}{d+1}\right)^{n_L}\right] if i \neq d \\ \frac{n_L}{i+1} if i = d \end{cases} \quad (23)$$

The goals of the multi-objective optimization approach should specify that the desired goal is to maximize the OEC objective function after taking into account all techno-economic elements. Also, the desired objective is considered for the two objective functions of BFC and LCC minimization. Also, the goal of the PMV objective function is to reach 0.

**Table 5**
Validation of Reverse Osmosis Desalination with the research of Nafey and Sharaf [62].

| Variable | Present study | Nafey [62] | Unit | Difference (%) |
|---|---|---|---|---|
| $\dot{W}_{pump,RO}$ | 1120 | 1131 | kW | 0.97 |
| $M_f$ | 485.9 | 485.9 | $m^3/h$ | 0 |
| SR | 0.9944 | 0.9944 | - | 0 |
| $X_b$ | 64,180 | 64,180 | Ppm | 0 |
| $X_d$ | 252 | 250 | Ppm | 0.8 |
| $\Delta P$ | 6843 | 6850 | kPa | 0.1 |

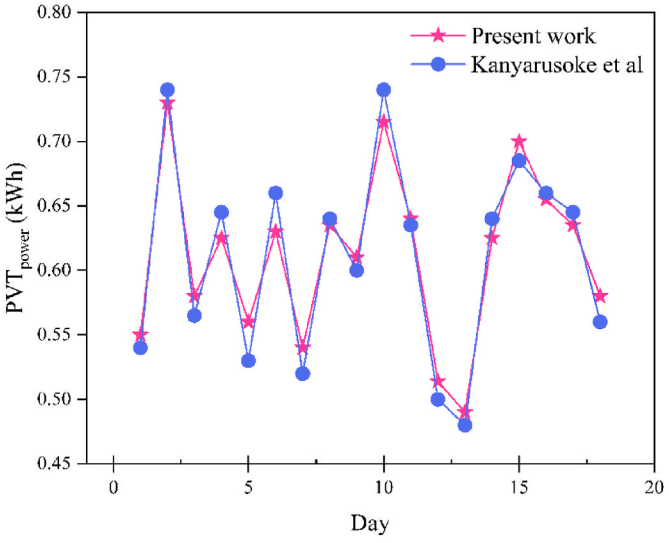


**Fig. 17.** Validation of the solar panel (PV/T) used in the proposed system [63].

## 5. Results

In this part, the results of modeling, optimization and performance of the system are discussed in the climatic conditions of different cities, and in the first step, the validation of the problem is discussed. It should be noted that problem modeling was done with TRNSYS software and problem optimization was done with response surface method (RSM) and Design Expert software.

### 5.1. Validation

Two reverse osmosis systems and a solar panel were chosen for validation in order to examine the simulation's accuracy. Because the system under review is a new and innovative system and is being reviewed for the first time, a validation is needed. The Nafey and Sharaf study [62] was used to verify the reverse osmosis desalination subsystem while taking into account the novel nature of the suggested system. The findings, which show high-accuracy modelling, are listed in Table 5. As the validation results show, this comparison has good validity and the error percentage of the two studies is very low.

The validation of PV/T panels represented in the TRNSYS software is

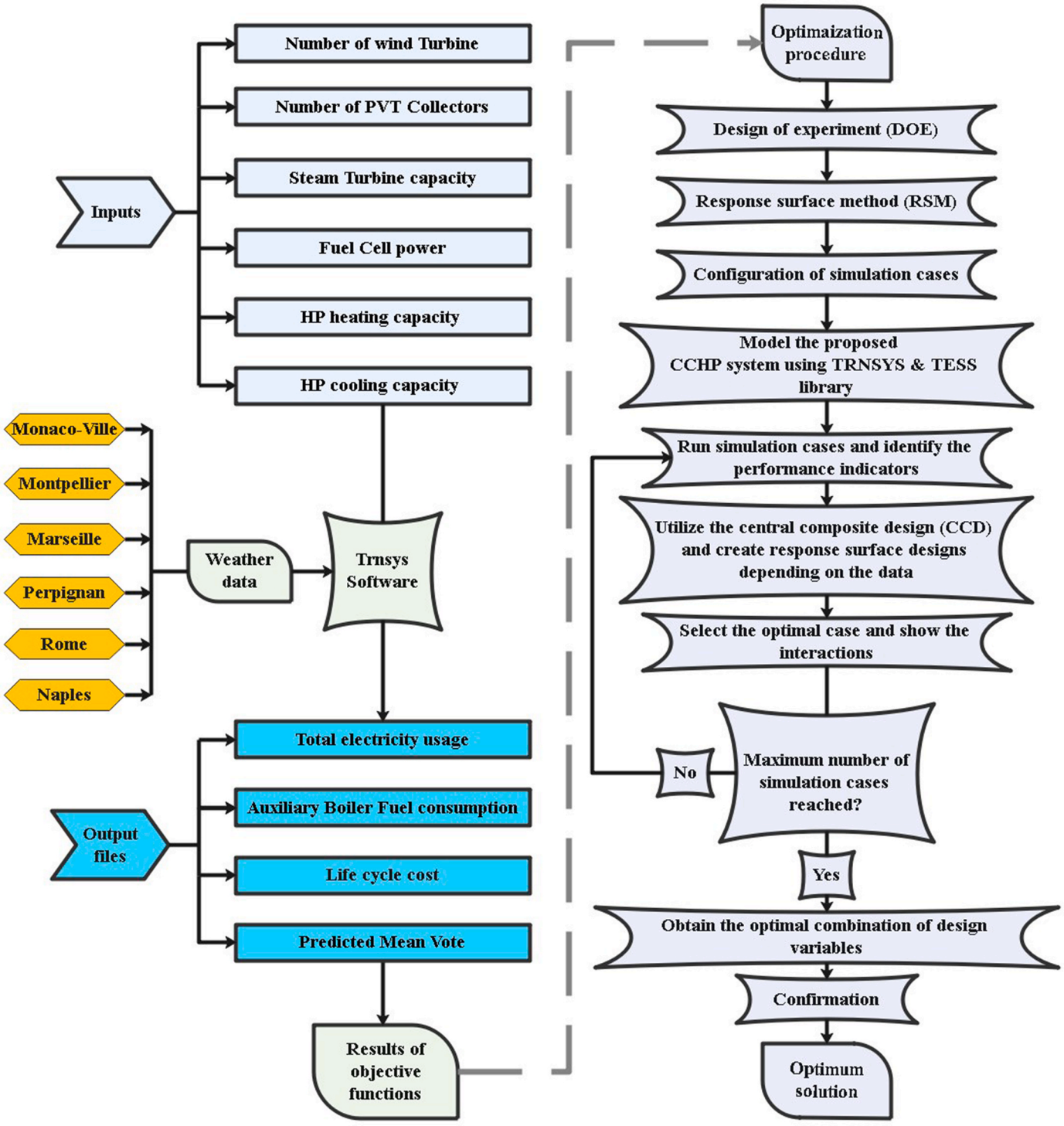


**Fig. 18.** Diagram of the optimization strategy.

**Table 6**
Maximum value of the selected governing design parameters.

| *case study* | *Number of PVT panels* | *Number of wind turbines* | *Steam turbine capacity (kW)* | *Fuel cell power (kW)* | *HP cooling capacity (kW)* | *HP heating capacity (kW)* |
|---|---|---|---|---|---|---|
| ***Marseille*** | *142* | *4* | *45.568* | *52.05* | *36.301* | *31.751* |
| ***Monaco*** | *162* | *5* | *38.7* | *42.638* | *49.499* | *51.979* |
| ***Montpellier*** | *185* | *6* | *65.881* | *70.175* | *57.451* | *46.046* |
| ***Naples*** | *135* | *5* | *73.504* | *37.685* | *57.029* | *26.887* |
| ***Perpignan*** | *134* | *3* | *44.244* | *44.889* | *46.561* | *36.845* |
| ***Rome*** | *198* | *7* | *67.982* | *61.82* | *36.552* | *41.169* |

**Table 7**
The most optimal points obtained for each of the studied cities.

| Performance metric | | OEC $\left(\frac{kWh}{year}\right)$ | BFC ($m^3$/year) $\left(\frac{m^3}{year}\right)$ | PMV (−) | LCC ($) |
|---|---|---|---|---|---|
| ***The optimal solution using the RSM*** | *Monaco* | *−29103.892* | *50476.6* | *0.206* | *334742.518* |
| | *Montpellier* | *−121217.314* | *47547.706* | *0.17* | *271734.064* |
| | *Marseille* | *−33671.568* | *51886.857* | *0.171* | *333487.677* |
| | *Perpignan* | *−20238.1* | *53458.12* | *0.165* | *352978.089* |
| | *Rome* | *−89777.437* | *47559.734* | *0.194* | *292892.946* |
| | *Naples* | *−9040.145* | *52430.463* | *0.25* | *366566.357* |
| ***Confirmation run*** | *Monaco* | *−27910.63243* | *48709.919* | *0.20188* | *318005.3921* |
| | *Montpellier* | *−116489.8388* | *46549.20417* | *0.16405* | *266027.6487* |
| | *Marseille* | *−32493.06312* | *50434.025* | *0.161937* | *328485.3618* |
| | *Perpignan* | *−18983.3378* | *51587.0858* | *0.16038* | *339211.9435* |
| | *Rome* | *−86365.89439* | *45657.34464* | *0.1843* | *280884.3352* |
| | *Naples* | *−8579.097605* | *49808.93985* | *0.24625* | *359968.1626* |
| ***Estimation error*** | *Monaco* | *4.1* | *3.5* | *2* | *5* |
| | *Montpellier* | *3.9* | *2.1* | *3.5* | *2.1* |
| | *Marseille* | *3.5* | *2.8* | *5.3* | *1.5* |
| | *Perpignan* | *6.2* | *3.5* | *2.8* | *3.9* |
| | *Rome* | *3.8* | *4* | *5* | *4.1* |
| | *Naples* | *5.1* | *5* | *1.5* | *1.8* |

shown in Fig. 17, which also demonstrates a fair degree of agreement between the current model and the research done by Kanyarusoke et al. [63]. As the validation results of the photovoltaic solar panel show, this comparison has been checked to check the amount of electricity produced in 20 days, the results indicate the good validity of this transient simulation and the error percentage of the two studies is very low.

### 5.2. Optimization

The interaction of numerous major design factors has an impact on hybrid systems, thus it's critical to build a technique for tracking how these interactions influence system performance indicators. The optimization technique used in this research sought to identify the optimum group of critical design parameters for the proposed cycle to achieve the best system efficiency from an energy and financial standpoint. Conventional optimization methods, however, have large computing costs and are unable to foresee the interactions between design elements and performance metrics [19]. A flowchart of the optimization technique used in this investigation is shown in Fig. 18. The first step in the design and optimization process is to determine the design points with tests, which are an effective tool for this issue.

Based on the results of the transient calculation, the RSM of optimization chooses the best configuration of the specified controller design variables, as shown in Table 4. Table 6 lists several values for the optimization factors for each city. A summary of the operating outcomes for the CCHP unit built using solar, wind, and geothermal energy sources are also included in Table 7. The calculation results were compared to the RSM's optimum settings to ensure the results were accurate. Make sure to optimize. Maximum error from the optimization procedure was 6.2 %. Table 7 shows the ultimate quantity of power generated, annual natural gas use, comfort rating, and system cost for each city individually.

The best city, which corresponds to Montpellier, is shown in Fig. 19's single-objective Pareto diagram along with the load distribution of modifications to the objective functions.

In the current research, the system's original design was initially carried out using wind, solar, and geothermal energy sources in accordance with the sites chosen and the availability of sufficient renewable energy capabilities in those places. The necessary subsystems were selected based on the demand for the production of products such as hot water and fresh water for the building, as well as the production of heating for the cold season and the production of cooling for the warm season, and the capacity of each subsystem was selected experimentally and with educational assumptions. The system's efficiency in terms of power production and cost was then assessed. In this phase, the system's performance for various cities was once again examined using the objective functions after optimizing and selecting the ideal spots for each area.According to Fig. 20, Montpellier, one of the six chosen cities, had the finest circumstances for the modelled and ideal system, having the maximum production capacity of −121217.314 (kWh/year), the lowest cost of 271734.064$, and the lowest quantity of gas consumption of 47547.706 m3/yaer. Naples had the poorest circumstances, both economically and in terms of producing energy, compared to the other six cities, with the greatest cost for the proposed system being 366566.357$ and the lowest output power of the system being −9040.145 (kWh/year) for Naples.

### 5.3. Comparison of electricity produced and consumed

The balance and equality of electricity generated and consumed are the most crucial factors to consider while developing the system, and the suggested system must be modelled in a manner that can accommodate consumption requirements at all times. A research was carried out to compare the power output of the system with the load used over the period of a whole year.

The results are shown in Fig. 21. Solar, wind, ST, and storage technologies might each provide a fraction of the system's annual power needs. These devices, however, are unable to consistently provide the necessary power throughout the day and night. The ST also contributed significantly to the yearly demand, as seen in Fig. 21, but this quantity was insufficient to fulfil the consumption requirement. The fact that additional support system is required in this case suggests that a fuel cell is the best option. The majority of annual power consumption demands and excess energy can be met by a fuel cell unit. Other significant factors in the selection and use of this unit in the current research include supplying the system expenses and selling the produced power to the net work.

In the proposed system, 4 power generation units including fuel cells, solar panels, wind turbine,s and steam turbines along with battery units for energy storage have been used to strengthen the electricity production and supply the energy consumption of the residential complex. The energy required by the solar panel is obtained from solar radiation, therefore any changes in the daily radiation of the sun affect the production of electricity and heat of the panel. On the other hand, the wind turbine works by wind energy, and any changes in the daily potential of wind energy affect the changes in the wind turbine's electricity production. On the other hand, the energy required for the steam turbine is obtained by geothermal energy. Unlike wind energy and solar energy, geothermal energy is a sustainable energy that can be used permanently and sustainably. For this reason, the production of electricity by the

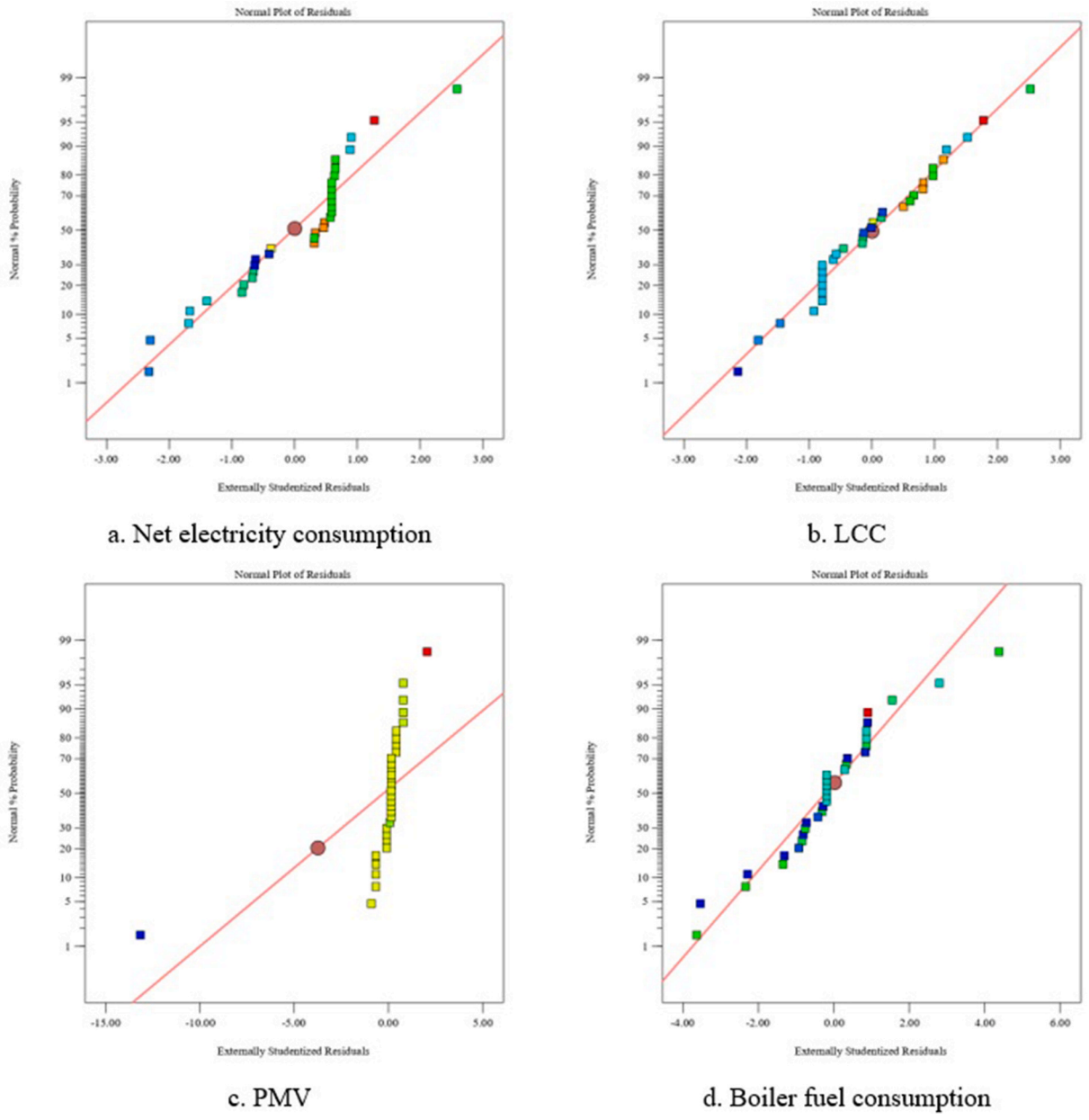


**Fig. 19.** Single-objective optimal results of the functions.

steam turbine is stable throughout the year, which is why the amount of electricity produced by this unit is more than the wind farm and the solar farm. The amount of electricity produced by the fuel cell is more than the whole unit, and the reason for this is the receipt of hydrogen and oxygen gas. As a result, the total power generation by all power generation units as well as the power stored in the battery is used to supply the electricity needed by the residential complex throughout the year, which is shown as load in Fig. 21.

### 5.4. Analysis of hot water produced

The system's ability to provide the necessary hot water for a year was another challenge. To create hot water, equipment that burns fossil fuels is often employed. As part of this research, efforts were made to reduce the amount of natural gas used to fuel the auxiliary boiler, which produces hot water. Additionally, solar energy was used to provide some of the system's hot water. As shown in Fig. 22, solar energy is insufficient to provide the system with all of the hot water it needs. Under some circumstances, solar energy can only supply a portion of the needed water up to a temperature of 32 °C, Therefore, the boiler is used to increase the thermal energy of the system to further increase the desired water temperature to the required level. The equipment used in this unit causes a 50 % increase in the temperature of the water fluid and this process has shown the activity of the fuel cell unit in preheating the required hot water. This equipment also had a direct impact on gas usage, lowering both prices and gas consumption. Reduce the system.

### 5.5. System dynamic performance

Montpellier, which had the best circumstances compared to the other six cities, had the dynamic performance of the suggested hybrid system shown in this section. The modelled system made use of several storage and renewable energy technologies. The total power used by the chosen apartment complex (red) and the total electricity generated by the system (blue) during a year are contrasted in Fig. 23. This outcome demonstrated that the suggested system provided the necessary power

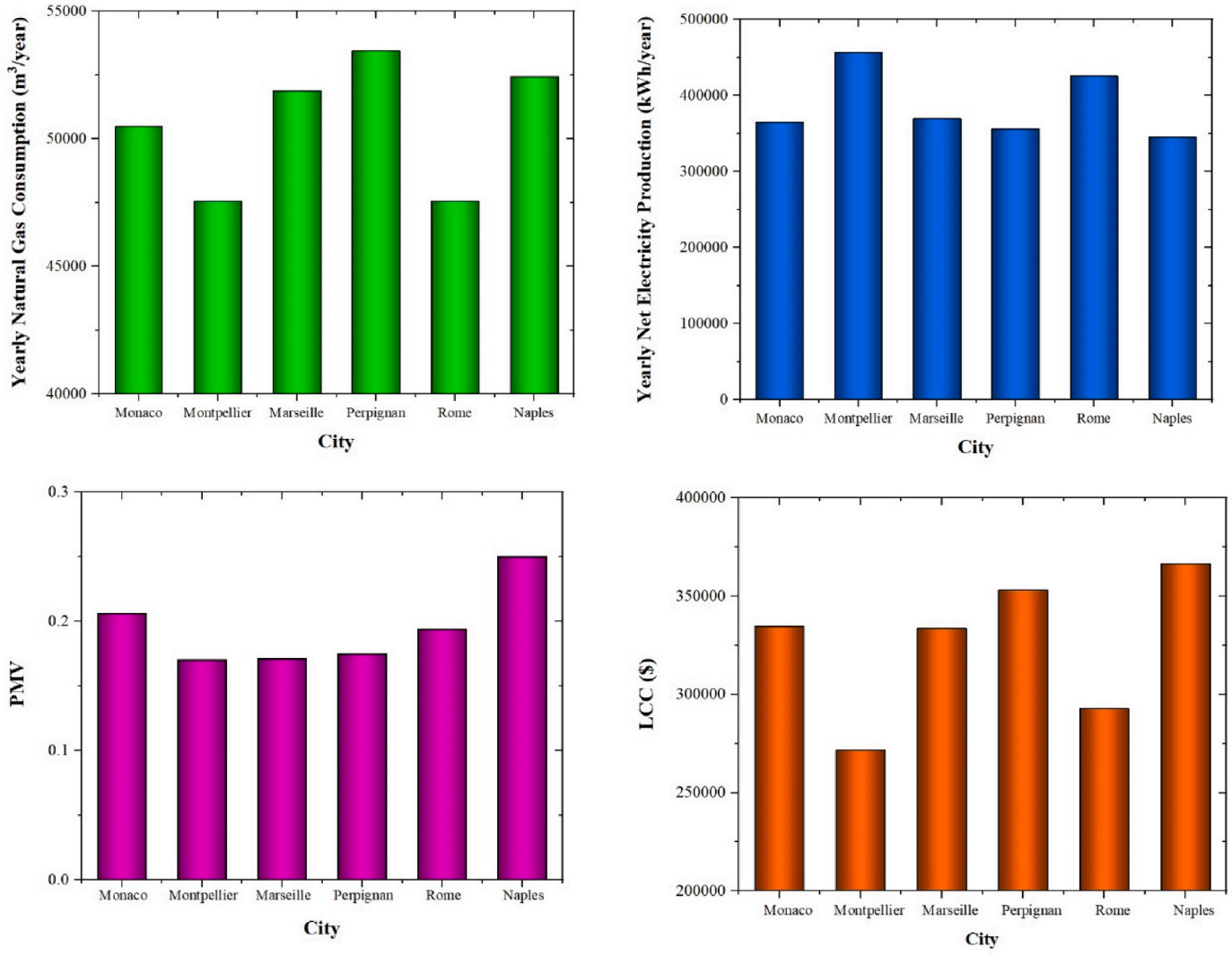


**Fig. 20.** Comparison of system performance of six cities after optimization.

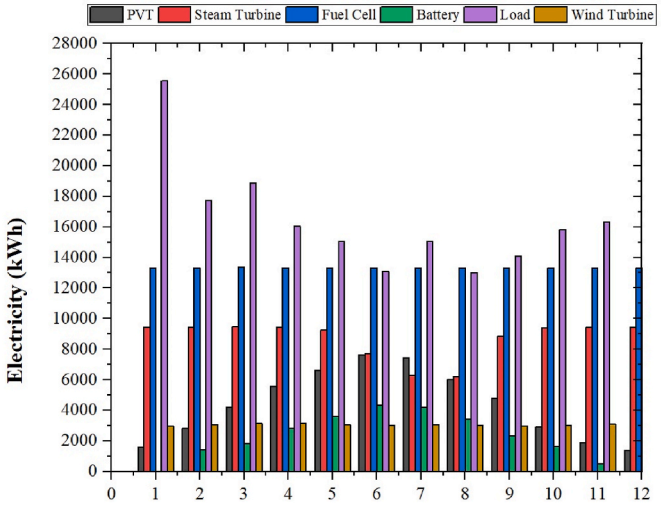


**Fig. 21.** comparing the units' electrical output and consumption.

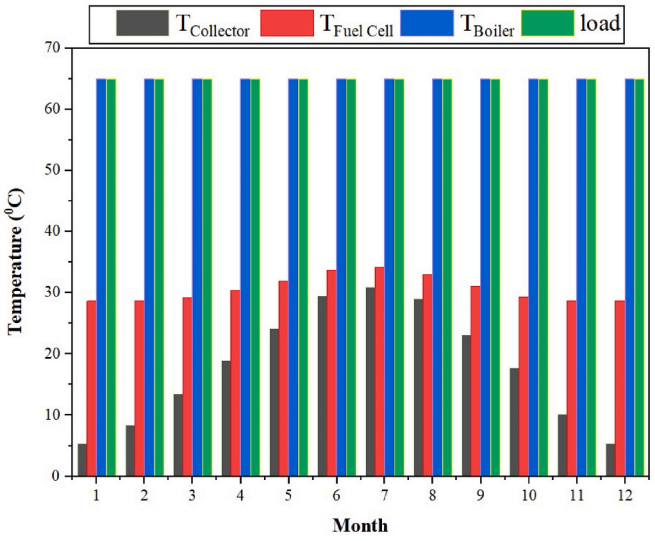


**Fig. 22.** Comparing the temperature and load of the system units.

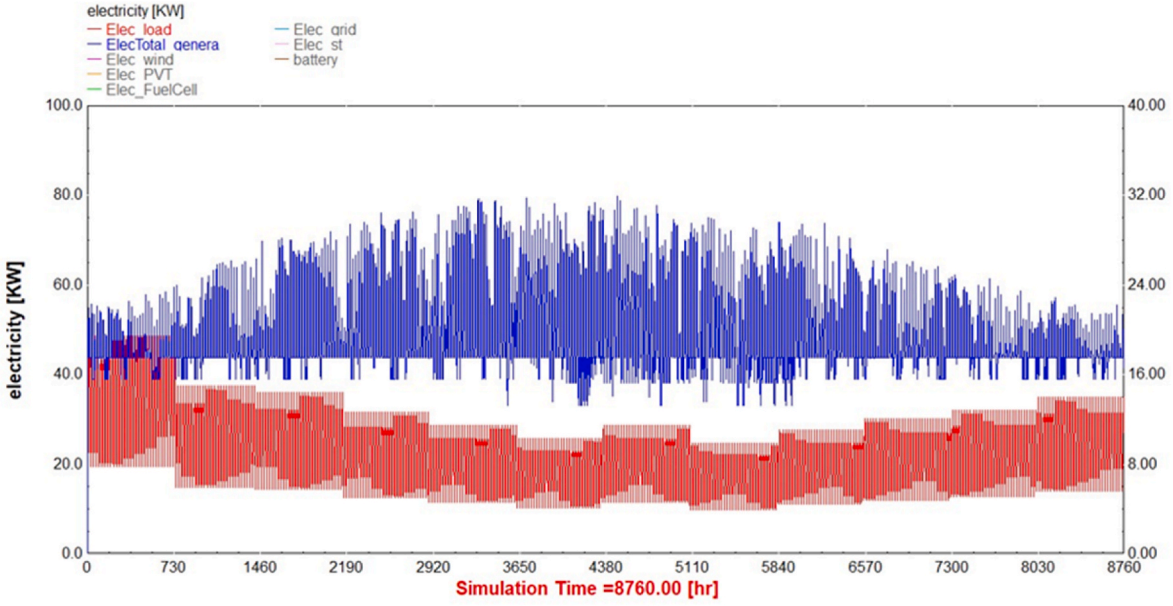


**Fig. 23.** Electricity produced and required by the residential unit throughout the year.

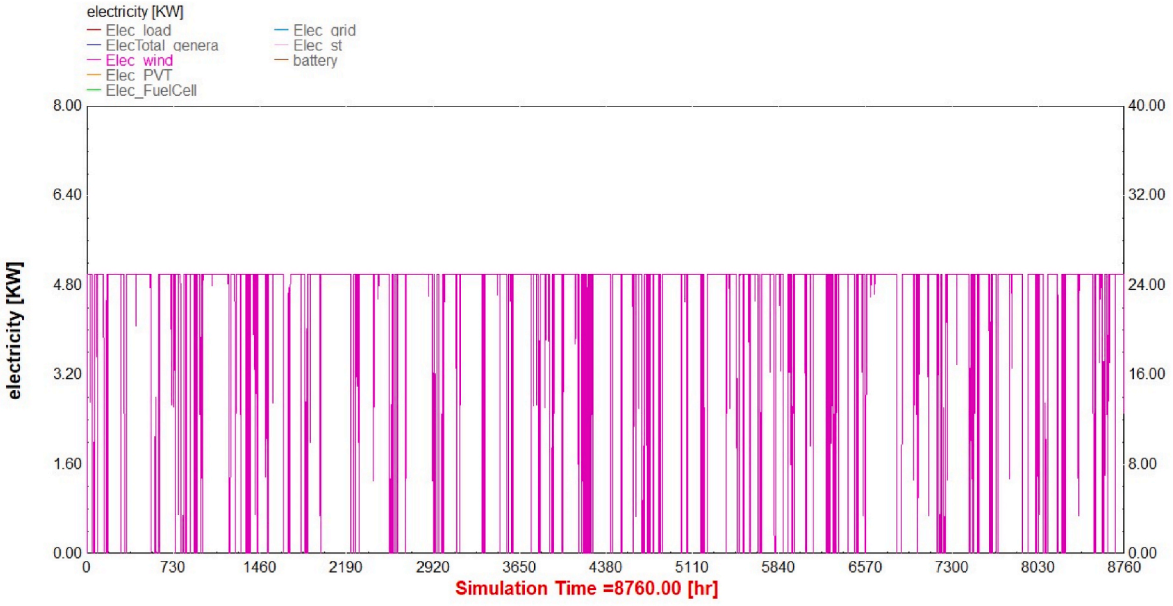


**Fig. 24.** Electricity produced by wind turbines.

throughout the whole year, day and night. Additionally, because there wasn't much of a discrepancy between the quantity of power generated and used, the excess was sold to the grid. As the results of this comparison show, during the year due to the increase in the absorption of solar energy and ambient temperature, and the absorption of more thermal energy for the production power system equipment, there is a greater increase in the summer season than in other seasons. Because with more thermal energy entering the solar panel, steam turbine and fuel cell, which are the three power generation units, the power increases. On the other hand, the amount of electricity load in the winter months is higher than in other months of the year due to the use of heating equipment.

The quantity of power generated by the WT, the last component of the system that provides energy, is seen in Fig. 24. The production power of wind turbines varies throughout the year and varies between 0 and 4.8 kW h, and it has a lower production capacity than other power generation units. It should be noted that wind turbines operate with changes in the wind speed of the environment and the production power of this unit depends on the changes in the speed of wind energy.

For the ease, speed, and accuracy of solving the problem of each building in calculating and determining the temperature of the building, it is necessary to divide the building into smaller and separate areas, and the most important factors that determine the boundaries of the zones are the use and area of the building. For this reason, to calculate the temperature of the building and then reach the predicted mean vote suitable for the building, the temperature analysis of the zones is effective in calculating the amount of electricity consumption and cooling and heating of the building. The selected apartment complex has four unique sections, as previously mentioned, the changes in indoor air temperature according to the demand of each selected section are shown

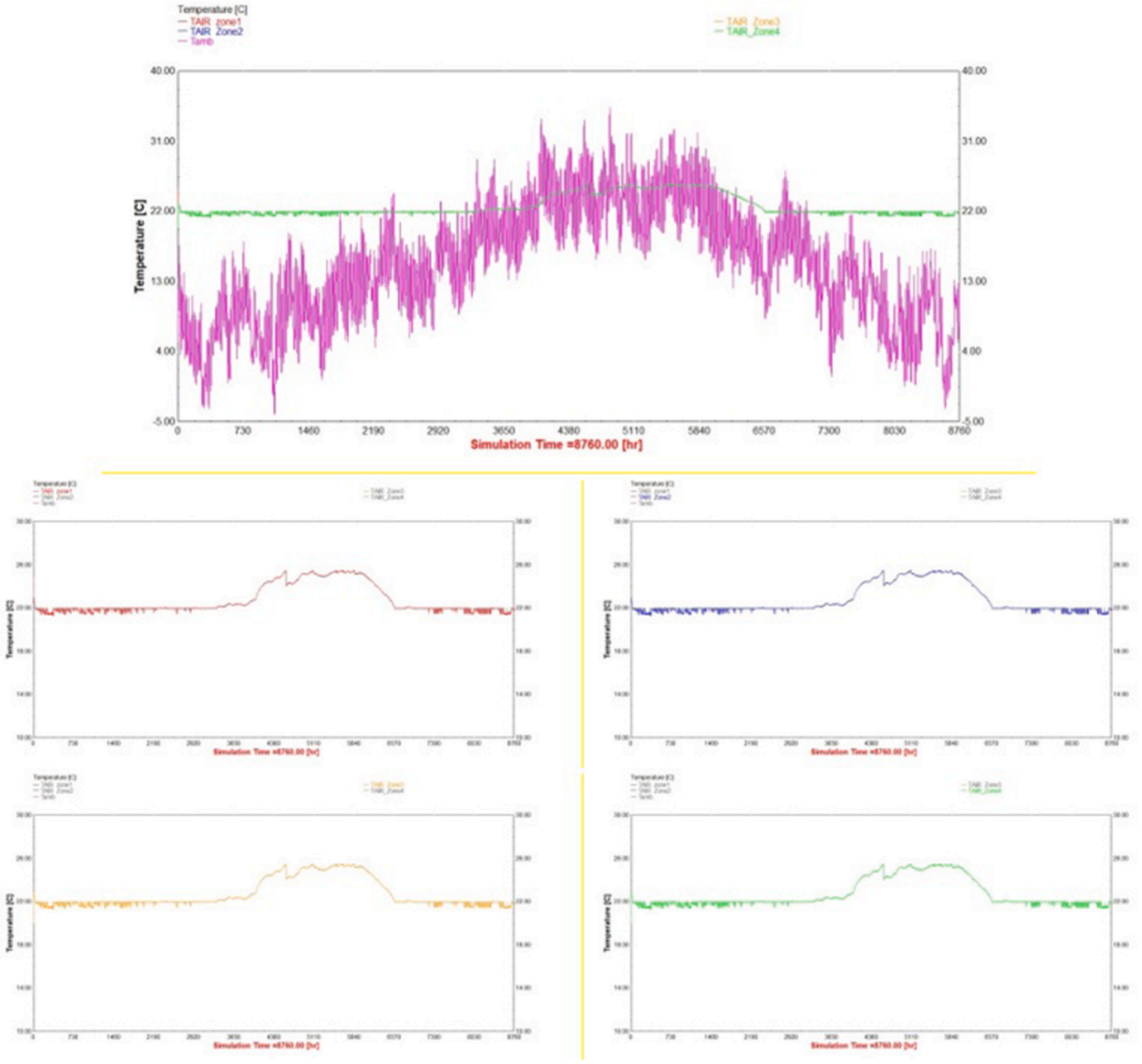


**Fig. 25.** Hourly temperature of the environment and of four zones of each building throughout the year.

in Fig. 25, which also shows the average hourly temperature of Montpellier in purple. The minimum air temperature is 20° Celsius and the maximum temperature is 26° Celsius, which shows that the planned system works well during the year. The results show that the highest temperature throughout the year for the best selected city occurs in the summer season and the months of June, July and August, and the lowest temperature throughout the year is in the months of January and December in the winter season. The results show that the temperature changes of the four selected zones in the building also change with the ambient temperature changes and the increase or decrease of the temperature of the zones is similar to the ambient temperature.

The suggested system's ability to deliver thermal comfort was assessed using PMV, as was previously mentioned. People feel warmer and colder depending on how positively or negatively the PMV number is skewed. The PMV's optimum value is zero, and interior conditions are improved with PMV levels that are near to zero. Fig. 26 displays the results of the PMV. As the results showed that in the hot months of the year, the value of PMV exceeds 0.4 and the value of PMV in the coldest months of the year is close to zero. The changes of PMV mode are similar to the changes of ambient temperature mode throughout the year and with the increase or decrease of ambient temperature.

The total volume of fresh water generated for the city of Montpellier over the course of a year, as shown in Fig. 27, was 3756.07 m3/year. The quantity of fresh water produced by the reverse osmosis desalination subsystem is presented hourly for a year in Fig. 27. The steam turbine's output power provides the electricity needed for the reverse osmosis desalination machine. The findings demonstrate that the amount of fresh water produced by the system grows with the amount of electricity produced during the summer months of the year increases, and decreases as the amount of power produced by the system increases.

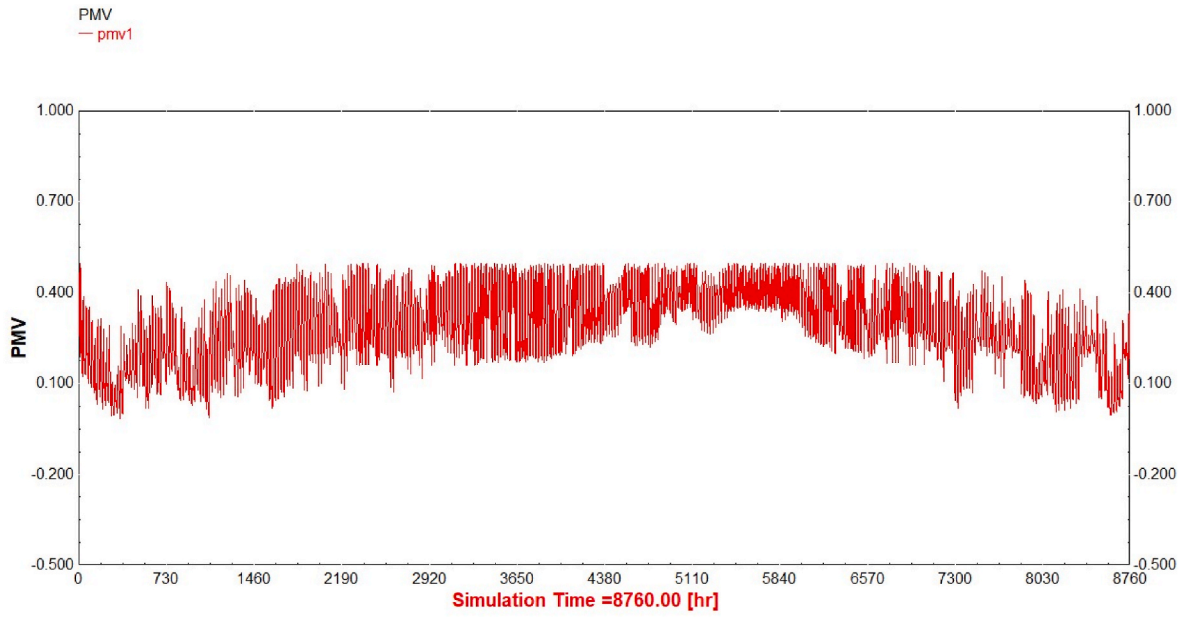


**Fig. 26.** Thermal comfort (PMV) for one year.

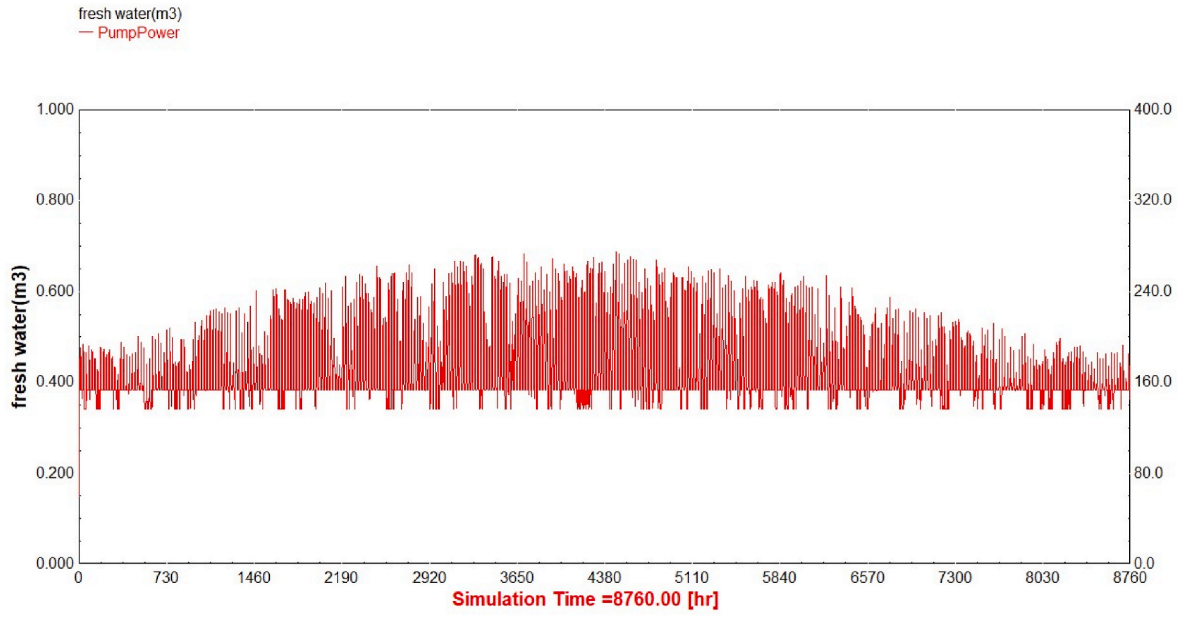


**Fig. 27.** Freshwater production throughout the year.

## 6. Conclusion

In this research, a system (CCHP) with wind, solar, and geothermal energy as energy sources, rechargeable batteries, and production of hydrogen were coupled and subjected to technical-economic analysis for 100 residential units in Marseille, Monaco, Montpellier, Naples, Perpignan, and Rome. Important components of the modelled system include WTs, STs, photovoltaic panels (PV/Ts), fuel cell circuits, HPs, reverse osmosis, electrolyzers, and hydrogen storage tanks. The RSM and TRNSYS software were utilized to analyze the design parameters of the primary CCHP controller. These parameters comprise the number of solar panels, the capacity of the ST, the number of wind turbines, the fuel cell unit capacity, and the cooling and heating capacity of the HP. Auxiliary boiler fuel use (BFC) and overall power consumption were the main indicators of Overall Electricity Consumption (OEC). The PMV was determined to be the thermal comfort score of the system, while the LCC served as the analysis's economic criterion. The original system design was chosen based on the use of electricity, cooling, heating, hot water, and freshwater subsystems by the cities chosen and the relevant capabilities of renewable energy in those locations. For the reliability of the necessary electrical and hot water supply, fuel cells must be used. The findings demonstrated that fuel cells, hydrogen generation and storage systems, and storage batteries play the most significant roles in the system's stability throughout the day and night. Montpellier was chosen after more research, system optimization, and analysis of the best city in terms of the volume of power generated, cost, and natural gas use. The total quantity of energy generated by the city's system in a year was 425690.937 (kWh), of which 121217.314 (kWh) were sold to the grid and the rest was used to power homes. The annual use of natural gas was 47547.706 $m^3$/year.

In summary, the results can be stated as follows.

- The results of multi-objective optimization with the response surface method showed that the system in Montpellier has 185 solar panels, 6 wind turbines, steam turbine capacity of 65.881 kW, fuel cell power of 70.175 kW, absorption chiller capacity of 57.451 kW and heat pump capacity of 46.046 kW.
- The results of multi-objective optimization with the response surface method showed that the optimal value of the objective functions OEC equals −121217.314 kWh/year, BFC equals 47547.706 m3, PMV equals 0.17 and LCC equals $271734.064.
- The transient simulation results showed that the optimal value of the objective functions PMV equals 0.16405 and LCC equals $266027.6487.
- The estimation error showed that the minimum and maximum error between the results of transient simulation and multi-objective optimization was between 2.1 and 3.9%.

## CRediT authorship contribution statement

**Ali Dezhdar:** Conceptualization, Methodology, Software, Visualization, Investigation. **Ehsanolah Assareh:** Conceptualization, Methodology, Software, Visualization, Investigation, Supervision, Writing – review & editing, Data curation. **Neha Agarwal:** Writing – review & editing. **Alireza Baheri:** Writing – review & editing. **Mehrdad Ahmadinejad:** Writing – review & editing. **Narjes Zadsar:** Writing – review & editing. **Ghazaleh Yeganeh Fard:** Writing – review & editing. **Ali bedakhanian:** Data curation. **Mona Aghajari:** Data curation, Software. **Maryam Ghodrat:** Writing – review & editing. **Mohammad Mafizur Rahman:** Writing – review & editing. **Moonyong Lee:** Supervision, Writing – review & editing.

## Declaration of competing interest

The authors declare that they have no known competing financial interests or personal relationships that could have appeared to influence the work reported in this paper.

## Acknowledgement

This work was supported by the National Research Foundation of Korea (NRF) grant funded by the Korea government (MSIT) (2021R1A2C1092152).

## References

[1] W. Wang, L. Fan, P. Zhou, Evolution of global fossil fuel trade dependencies, Energy 238 (2022), 121924.
[2] Ehsanolah Assareh, Mohammad Assareh, Seyed Mojtaba Alirahmi, Saeid Jalilinasrabady, Dejdar Ali, Mohsen Izadi, An extensive thermo-economic evaluation and optimization of an integrated system empowered by solar-wind-ocean energy converter for electricity generation – case study: Bandar Abas, Iran, Therm. Sci. Eng. Prog. 25 (2021), 100965. ISSN 2451-9049.
[3] B. Mendecka, R. Cozzolino, M. Leveni, G. Bella, Energetic and exergetic performance evaluation of a solar cooling and heating system assisted with thermal storage, Energy 176 (2019) 816–829.
[4] I.B. Fridleifsson, Status of geothermal energy amongst the world's energy sources, Geothermics 32 (2003) 379e88.
[5] D. Moya, C. Ald' as, P. Kaparaju, Geothermal energy: power plant technology and direct heat applications, Renew. Sustain. Energy Rev. 94 (2018) 889–901.
[6] M.A. Bagherian, K. Mehranzamir, A.B. Pour, S. Rezania, E. Taghavi, H. Nabipour-Afrouzi, et al., Classification and analysis of optimization techniques for integrated energy systems utilizing renewable energy sources: a review for CHP and CCHP systems, Processes 9 (2021) 339.
[7] K. Chen, M. Pan, Operation optimization of combined cooling, heating, and power superstructure system for satisfying demand fluctuation, Energy 237 (2021), 121599.
[8] D.W. Wu, R.Z. Wang, Combined cooling, heating and power: a review, Prog. Energy Combust. Sci. 32 (2006) 459–495.
[9] S. Kavian, C. Aghanajafi, H.J. Mosleh, A. Nazari, A. Nazari, Exergy, economic and environmental evaluation of an optimized hybrid photovoltaic-geothermal heat pump system, Appl. Energy 276 (2020), 115469.
[10] X. Wang, Y. Xu, Z. Fu, J. Guo, Z. Bao, W. Li, et al., A dynamic interactive optimization model of CCHP system involving demand-side and supply-side impacts of climate change. Part I: methodology development, Energy Convers. Manag. 252 (2022), 115112.
[11] F. Ren, Z. Wei, X. Zhai, Multi-objective optimization and evaluation of hybrid CCHP systems for different building types, Energy 215 (2021), 119096.
[12] F. Musharavati, S. Khanmohammadi, A. Pakseresht, A novel multi-generation energy system based on geothermal energy source: thermo-economic evaluation and optimization, Energy Convers. Manag. 230 (2021), 113829.
[13] N. Li, X. Zhao, X. Shi, Z. Pei, H. Mu, F. Taghizadeh-Hesary, Integrated energy systems with CCHP and hydrogen supply: a new outlet for curtailed wind power, Appl. Energy 303 (2021), 117619.
[14] N. Mahdavi, P. Mojaver, S. Khalilarya, Multi-objective optimization of power, CO2 emission and exergy efficiency of a novel solar-assisted CCHP system using RSM and TOPSIS coupled method, Renew. Energy 185 (2022) 506–524.
[15] A. Dezhdar, et al., A Transient Model for Clean Electricity Generation Using Solar Energy and Ocean Thermal Energy Conversion (OTEC) - Case Study: Karkheh Dam - Southwest Iran, Energy Nexus, 2023, 100176.
[16] C. Chen, Q. Xia, S. Feng, Q. Liu, A novel solar hydrogen production system integrating high temperature electrolysis with ammonia based thermochemical energy storage, Energy Convers. Manag. 237 (2021), 114143.
[17] A.A. Alrobaian, Energy, exergy, economy, and environmental (4E) analysis of a multi-generation system composed of solar-assisted Brayton cycle, Kalina cycle, and absorption chiller, Appl. Therm. Eng. 204 (2022), 117988.
[18] S. Saikia, V. Verma, B.K. Kakati, T. Sivasakthivel, R. Tarodiya, Optimization of solar integrated electrolyser system for hydrogen production using Taguchi method, Mater. Today Proc. 49 (2021) 397–402.
[19] M. Ji, et al., Optimisation of multi-period renewable energy systems with hydrogen and battery energy storage: a P-graph approach, Energy Convers. Manag. 281 (2023), 116826.
[20] A.F. Güven, O.Ö. Mengi, Assessing metaheuristic algorithms in determining dimensions of hybrid energy systems for isolated rural environments: Exploring renewable energy systems with hydrogen storage features, J. Clean. Prod. 428 (2023), 139339.
[21] B. Modu, et al., A systematic review of hybrid renewable energy systems with hydrogen storage: sizing, optimization, and energy management strategy, Int. J. Hydrogen Energy. 48 (2023) 38354–38373.
[22] L. Liu, et al., Performance evaluation of wind-solar-hydrogen system for renewable energy generation and green hydrogen generation and storage: energy, exergy, economic, and enviroeconomic, Energy 276 (2023), 127386.
[23] M. Abedi, et al., Solar desalination chimneys: investigation on the feasibility of integrating solar chimneys with humidification–dehumidification systems, Renew. Energy 202 (2023) 88–102.
[24] N. Khani, et al., 6E analyses of a new solar energy-driven polygeneration system integrating CO2 capture, organic Rankine cycle, and humidification-dehumidification desalination, J. Clean. Prod. 379 (2022), 134478.
[25] M. Tawalbeh, et al., Analysis for hybrid photovoltaic/solar chimney seawater desalination plant: a CFD simulation in Sharjah, United Arab Emirates, Renew. Energy 202 (2023) 667–685.
[26] E. Assareh, et al., A transient simulation for a novel solar-geothermal cogeneration system with a selection of heat transfer fluids using thermodynamics analysis and ANN intelligent (AI) modeling, Appl. Therm. Eng. 231 (2023), 120698.
[27] Ehsanolah Assareh, Dejdar Ali, Ershadi Ali, Masoud Jafarian, Mohammadhossein Mansouri, Amir Salek roshani, Ehsan Azish, Ehsan Saedpanah, Moonyong Lee, Techno-economic analysis of combined cooling, heating, and power (CCHP) system integrated with multiple renewable energy sources and energy storage units, Energy Build. 278 (2023), 112618. ISSN 0378-7788.
[28] G. A' lvarez, M. Chagolla, J. Xama' n, M. Jime' nez, S. Sua' rez, M. Heras, A TRNSYS simulation and experimental comparison of the thermal behavior of a building located in Desert climate, Energy Sustainability (2010) 349–356.
[29] J.F. Kreider, F. Kreith, Solar Energy Handbook, 1981.
[30] W. Yaïci, E. Entchev, K. Lombardi, Experimental and simulation study on a solar domestic hot water system with flat-plate collectors for the Canadian climatic conditions, Energy Sustainability. American Society of Mechanical Engineers (2012) 69–78.
[31] Y. Allard, M. Kummert, M. Bernier, A. Moreau, Intermodel comparison and experimental validation of electrical water heater models in TRNSYS, Proceedings of Building Simulation (2011) 688–695.
[32] D. Brough, J. Ramos, B. Delpech, H. Jouhara, Development and validation of a TRNSYS type to simulate heat pipe heat exchangers in transient applications of waste heat recovery, International Journal of Thermofluids 9 (2021), 100056.
[33] M. Rezvanpour, D. Borooghani, F. Torabi, M. Pazoki, Using CaCl2· 6H2O as a phase change material for thermo-regulation and enhancing photovoltaic panels' conversion efficiency: experimental study and TRNSYS validation, Renew. Energy 146 (2020) 1907–1921.
[34] S.A. Kalogirou, R. Agathokleous, G. Barone, A. Buonomano, C. Forzano, A. Palombo, Development and validation of a new TRNSYS Type for thermosiphon flat-plate solar thermal collectors: energy and economic optimization for hot water production in different climates, Renew. Energy 136 (2019) 632–644.
[35] Y. Cao, H.A. Dhahad, H. Togun, A. El-Shafay, S. Alamri, A.A. Rajhi, et al., Development and transient performance analysis of a decentralized grid-connected smart energy system based on hybrid solar-geothermal resources; Techno-economic evaluation, Sustain. Cities Soc. 76 (2022), 103425.
[36] N. Sommerfeldt, P. Ollas, Reverse Engineering Prototype Solar PV/thermal Collector Properties from Empirical Data for Use in TRNSYS Type 560. ISES Solar World Congress and IEA Solar Heating and Cooling Conference 2017, UAE, Abu Dhabi, 2017, pp. 1121–1132. October 29-November 2, 2017.

[37] A. Buonomano, F. Calise, M.D. d'Accadia, M. Vicidomini, A hybrid renewable system based on wind and solar energy coupled with an electrical storage: dynamic simulation and economic assessment, Energy 155 (2018) 174–189.
[38] H. Kim, J. Baltazar, J. Haberl, Methodology for Calculating Cooling and Heating Energy-Imput-Ratio (EIR) from the Rated Seasonal Performance Efficiency (SEER or HSPF), 2013.
[39] TESS. Component Libraries v, 17.01 for TRNSYS V17. 0 and the TRNSYS Simulation Studio, Parameter/Input/Output Reference Manual, Thermal Energy System Specialists, LLC, 2004.
[40] S. Klein, B. Newton, J. Thornton, D. Bradley, J. Mitchell, M. Kummert, TRNSYS Reference Manual: Mathematical Reference, 2006.
[41] F. Oueslati, Hybrid renewable system based on solar wind and fuel cell energies coupled with diesel engines for Tunisian climate: TRNSYS simulation and economic assessment, Int. J. Green Energy 18 (2021) 402–423.
[42] R.F. Asrami, A. Sohani, E. Saedpanah, H. Sayyaadi, Towards achieving the best solution to utilize photovoltaic solar panels for residential buildings in urban areas, Sustain. Cities Soc. 71 (2021), 102968.
[43] E. Saedpanah, R.F. Asrami, A. Sohani, H. Sayyaadi, Life cycle comparison of potential scenarios to achieve the foremost performance for an off-grid photovoltaic electrification system, J. Clean. Prod. 242 (2020), 118440.
[44] H. Ashidi, J. Khorshidi, Exergoeconomic analysis and optimization of a solar based hybrid system using multiobjective differential evolution algorithm, J. Clean. Prod. 170 (2018) 978–990, 45.
[45] A. Nemati, M. Sadeghi, M. Yari, Exergoeconomic analysis and multi-objective optimization of a marine engine waste heat driven RO desalination system integrated with an organic Rankine cycle using zeotropic working fluid, Desalination 422 (2017) 113–123, 2017. 46.
[46] A. Naseri, M. Bidi, M.H. Ahmadi, R. Saidur, Exergy analysis of a hydrogen and water production process by a solar-driven transcritical CO2 power cycle with Stirling engine, J. Clean. Prod. 158 (2017) 165–181.
[47] M. Dongellini, G.L. Morini, On-off cycling losses of reversible air-to-water heat pump systems as a function of the unit power modulation capacity, Energy Convers. Manag. 196 (2019) 966–978.
[48] K. Fong, C. Lee, Solar desiccant cooling system for hot and humid region–A new perspective and investigation, Sol. Energy 195 (2020) 677–684.
[49] S.-H. Park, Y.-S. Jang, E.-J. Kim, Multi-objective optimization for sizing multi-source renewable energy systems in the community center of a residential apartment complex, Energy Convers. Manag. 244 (2021), 114446.
[50] E. Assareh, et al., Performance analysis of solar-assisted-geothermal combined cooling, heating, and power (CCHP) systems incorporated with a hydrogen generation subsystem, J. Build. Eng. 65 (2023), 105727.
[51] A. Dezhdar, et al., Transient optimization of a new solar-wind multi-generation system for hydrogen production, desalination, clean electricity, heating, cooling, and energy storage using TRNSYS, Renew. Energy 208 (2023) 512–537.
[52] S. Rayegan, S. Motaghian, G. Heidarinejad, H. Pasdarshahri, P. Ahmadi, M. A. Rosen, Dynamic simulation and multi-objective optimization of a solar-assisted desiccant cooling system integrated with ground source renewable energy, Appl. Therm. Eng. 173 (2020), 115210.
[53] A. Sohani, H. Sayyaadi, Thermal comfort based resources consumption and economic analysis of a two-stage direct-indirect evaporative cooler with diverse water to electricity tariff conditions, Energy Convers. Manag. 172 (2018) 248–264.
[54] A. Heidari, R. Roshandel, V. Vakiloroaya, An innovative solar assisted desiccant-based evaporative cooling system for co-production of water and cooling in hot and humid climates, Energy Convers. Manag. 185 (2019) 396–409.
[55] M.S. Saleem, N. Abas, A.R. Kalair, S. Rauf, A. Haider, M.S. Tahir, et al., Design and optimization of hybrid solar-hydrogen generation system using TRNSYS, Int. J. Hydrogen Energy 45 (2020) 15814–15830.
[56] N. Sommerfeldt, H. Madani, In-depth techno-economic analysis of PV/Thermal plus ground source heat pump systems for multi-family houses in a heating dominated climate, Sol. Energy 190 (2019) 44–62.
[57] M. Dongellini, G.L. Morini, On-off cycling losses of reversible air-to-water heat pump systems as a function of the unit power modulation capacity, Energy Convers. Manag. 196 (2019) 966–978.
[58] A. Sohani, H. Sayyaadi, M. Azimi, Employing static and dynamic optimization approaches on a desiccant-enhanced indirect evaporative cooling system, Energy Convers. Manag. 199 (2019), 112017.
[59] R. Ghelich, M.R. Jahannama, H. Abdizadeh, F.S. Torknik, M.R. Vaezi, Central composite design (CCD)-Response surface methodology (RSM) of effective electrospinning parameters on PVP-B-Hf hybrid nanofibrous composites for synthesis of HfB2-based composite nanofibers, Compos. B Eng. 166 (2019) 527–541.
[60] Design Expert Software, V 13.0.5, Stat-Ease Inc, Minneapolis (USA), 2021.
[61] P.O. Fanger, Thermal Comfort. Analysis and Applications in Environmental Engineering. Thermal Comfort Analysis and Applications in Environmental Engineering, 1970.
[62] A.S. Nafey, M.A. Sharaf, Combined solar organic Rankine cycle with reverse osmosis desalination process: energy, exergy, and cost evaluations, Renew. Energy 35 (2010) 2571–2580.
[63] K. Kanyarusoke, J. Gryzagoridis, G. Oliver, Validation of TRNSYS modelling for a fixed slope photovoltaic panel, Turk. J. Electr. Eng. Comput. Sci. 24 (6) (2016) 4763–4772.
[64] Broad overview of energy efficiency and renewable energy opportunities for Department of Defense installations - scientific figure on ResearchGate. Available from: https://www.researchgate.net/figure/Temperature-for-Europe-at-5-km-depth-European-Deep-Geothermal-Energy-Programme-2010_fig5_255380937 [accessed 12 November, 2022].
[65] Globalsolaratlas, GSA 2.9, September 2023. www.globalsolaratlas.info.
[66] The Global Wind Atlas, globalwindatlas.info.